

Effect of phosphodiesterase 10 inhibition on pulmonary smooth muscle cell proliferation
and signaling pathways

Inaugural Dissertation

Submitted to the Faculty of Medicine

In partial fulfillment for the requirements

for the degree of Doctor of Medicine

in the Faculty of Medicine

of the Justus Liebig University of Giessen

by Caroline Merkel

from Oberkirch, Germany

Gießen 2020

Aus dem Fachbereich Medizin der Justus-Liebig-Universität Gießen

Excellence Cluster Cardio-Pulmonary System Gießen

Gutachter: Prof. Dr. rer. nat. Ralph T.

Schermuly Gutachter: Prof. Dr. R. Savai

Tag der Disputation: 20. Juli 2021

INDEX

Index

INDEX	I
LIST OF FIGURES	II
LIST OF TABLES	III
ABBREVIATIONS.....	IV
1 INTRODUCTION	1
1.1 PULMONARY HYPERTENSION.....	1
1.1.1 <i>Definition and diagnosis of pulmonary hypertension</i>	1
1.1.2 <i>Classification of pulmonary hypertension</i>	1
1.2 PULMONARY ARTERIAL HYPERTENSION.....	3
1.2.1 <i>Pathogenesis and molecular mechanisms</i>	3
1.2.2 <i>Histopathology of pulmonary arterial hypertension</i>	6
1.2.3 <i>Treatment of pulmonary arterial hypertension</i>	8
1.3 PHOSPHODIESTERASE	11
1.3.1 <i>Cyclic nucleotides</i>	11
1.3.2 <i>Cyclic nucleotide phosphodiesterases</i>	13
1.3.3 <i>Phosphodiesterase 10 family</i>	16
1.3.4 <i>The role of phosphodiesterase 10A in pulmonary arterial hypertension</i>	17
2 AIMS OF THE STUDY	19
3 MATERIAL AND METHODS	21
3.1 MATERIAL.....	21
3.1.1 <i>Chemicals, reagents and kits</i>	21
3.1.2 <i>Phosphodiesterase 10 inhibitor</i>	22
3.1.3 <i>Cell culture</i>	22
3.1.4 <i>Antibodies</i>	22
3.1.5 <i>Equipment</i>	23
3.1.6 <i>Other Materials</i>	23
3.2 METHODS.....	24
3.2.1 <i>Animal model</i>	24
3.2.2 <i>Cell culture with human pulmonary arterial muscle cells</i>	27
3.2.3 <i>Statistical Analysis</i>	31
4 RESULTS.....	32

INDEX

4.1	EFFECT OF PHOSPHODIESTERASE 10 INHIBITION ON HUMAN PULMONARY ARTERIAL SMOOTH MUSCLE CELL PROLIFERATION AND SIGNALING.....	32
4.1.1	<i>Characterization of phosphodiesterase 10 induced proliferation in human pulmonary arterial smooth muscle cell.....</i>	32
4.1.2	<i>Effect of phosphodiesterase 10 inhibition on cell cycle in human pulmonary arterial smooth muscle cells.....</i>	33
4.1.3	<i>Protein kinase A/cAMP element binding protein-axis.....</i>	35
4.2	EFFECT OF PHOSPHODIESTERASE 10 INHIBITION IN MONOCROTALINE RAT MODEL.....	37
4.2.1	<i>Histological assessment of treatment effect of phosphodiesterase 10 inhibition.....</i>	37
4.2.2	<i>Effects of phosphodiesterase 10 inhibition on hemodynamic parameters in monocrotaline rat model.....</i>	40
4.2.3	<i>Effect of phosphodiesterase 10 inhibition on right heart function.....</i>	42
5	DISCUSSION	46
5.1	RESULTS	46
5.1.1	<i>Pulmonary arterial smooth muscle cells in patients with pulmonary arterial hypertension are hyperproliferative.....</i>	46
5.1.2	<i>Molecular mechanisms mediating phosphodiesterase 10-induced proliferation</i>	47
5.1.3	<i>Therapeutic effect of phosphodiesterase 10 inhibition in monocrotaline rat model</i>	49
5.2	LIMITATIONS.....	50
5.3	CONCLUSION AND PERSPECTIVES	51
6	DECLARATION.....	53
7	REFERENCES.....	54

LIST OF FIGURES

LIST OF FIGURES

- Figure 1 Vascular remodeling in pulmonary arterial hypertension
- Figure 2 Pathobiology of PAH
- Figure 3 Histology of PAH
- Figure 4 Endothelial dysfunction in pulmonary arterial hypertension and current therapeutic target therapies
- Figure 5 Cyclic nucleotide signaling pathway
- Figure 6 Cyclic nucleotide hydrolysis by cyclic nucleotide phosphodiesterases
- Figure 7 Nomenclature of PDE
- Figure 8 Structure of 11 PDE family members
- Figure 9 PDE mRNA expression in lung vasculature in rat
- Figure 10 Study design
- Figure 11 Tricuspid annular plane systolic excursion
- Figure 12 FCS-induced cell proliferation of hPASMC
- Figure 13 PDGF-induced cell proliferation of hPASMC
- Figure 14 Influence of PDE10 on p27, p21 and cyclin D
- Figure 15 PDE10 inhibition reverses PDGF-induced stimulation of cyclin D in hPASMCs
- Figure 16 Increase of pCREB by PDE10 inhibition
- Figure 17 Increase of PKA by PDE10 inhibition
- Figure 18 PPAR γ expression in donor and IPAH hPASMC
- Figure 19 Effect of PDE10 inhibition on degree of muscularization
- Figure 20 Medial wall thickness
- Figure 21 Effect of PDE10 inhibition on right ventricular systolic pressure on MCT-PH rats
- Figure 22 Systemic arterial pressure and heart rate during measurement

LIST OF FIGURES

- Figure 23 Tricuspid annular plane systolic excursion
- Figure 24 Effect of PDE10 inhibition on right ventricular hypertrophy on MCT-PH rats
- Figure 25 Cardiac index in ml/min/100 g body weight
- Figure 26 cAMP/PKA/CREB axis

LIST OF TABLES

LIST OF TABLES

Table 1	Updated clinical classification of PH (Nice, 2018)
Table 2	Cyclic nucleotide phosphodiesterase isozyme families
Table 3	SDS sample buffer
Table 4	Running buffer
Table 5	Blotting buffer
Table 6	Stacking gel
Table 7	Separating gel
Table 8	Nonfat milk
Table 9	TSBT

ABBREVIATIONS

ABBREVIATIONS

AMP	Adenosine monophosphate
cAMP	Cyclic adenosine monophosphate
cDNA	Complementary desoxyribonucleic acid
cGMP	Cyclic guanosine monophosphate
CNG	Cyclic nucleotide-gated channel
CREB	cAMP-response element-binding protein
Ct	Cycle threshold
BW	Bodyweight
DPBS	Dulbecco's phosphate buffered saline
ECL	Enhanced chemiluminescence
EPAC	Exchange protein directly activated by cAMP
ERA	Endothelin receptor antagonist
ETA	Endothelin receptor A
ETB	Endothelin receptor B
ET-1	Endothelin-1
<i>et al.</i>	<i>et alii</i> (and others)
FCS	Fetal calf serum
GAF	cGMP-specific phosphodiesterases, adenylyl cyclases, FhIA
GAPDH	Glyceraldehyde 3-phosphate dehydrogenase
GMP	Guanosine monophosphate
h	hours
HCL	Hydrogen chloride
hPASMC	Human pulmonary arterial smooth muscle cell
IL-1	Interleukin 1
IL-6	Interleukin 6
IPAH	Idiopathic pulmonary arterial hypertension
kDa	Kilodalton
kg	Kilogram
LV	Left ventricle
MCT	Monocrotaline
NaOH	Sodium hydroxide
NO	Nitric oxide
NTC	Non-treated cells
RNA	Ribonucleic acid

ABBREVIATIONS

PAH	Pulmonary arterial hypertension
PAP	Pulmonary arterial pressure
PASMC	Pulmonary arterial smooth muscle cell
PASP	Pulmonary arterial systolic pressure
pCREB	Phosphorylated cAMP-response element-binding protein
PDE	Phosphodiesterase
PDGF	Platelet derived growth factor
PH	Pulmonary hypertension
PKA	Protein kinase A
PKG	Protein kinase G
PPAR	Peroxisome proliferator-activated receptor
qRT-PCR	Quantitative real time- polymerase chain reaction
RHC	Right heart catheter
RIPA buffer	Radioimmunoprecipitation assay buffer
RV	Right ventricle
RVSP	Right ventricular systolic pressure
SDS	Sodium dodecyl sulfate
SEM	Standard error of the mean
SMC	Smooth muscle cell
TAPSE	Tricuspid annular plane systolic excursion
TBST	Tris-buffered saline and tween
TEMED	Tetramethyl ethylenediamine
TGF	Transforming growth factor
Tris	Tris-(hydroxy methyl)-amino methane
vs	<i>versus</i>
5-HT	Serotonin, 5-hydroxytryptamin

SUMMARY

SUMMARY

Pulmonary arterial hypertension (PAH) is a progressive lung disease due to contraction of arteries and remodeling leading to increased resistance and increased blood pressure in lung circulation. Genesis of the disease is promoted by up or down regulation of many mediators. Two of those mediators are believed to be the second messengers cyclic adenosine monophosphate (cAMP) and cyclic guanosine monophosphate (cGMP). The amounts of these second messengers were found to be decreased in experimental studies and in PAH patients. The degradation of cAMP and cGMP is regulated by phosphodiesterases (PDE). PDE reduce second messenger levels and thus favor PAH. Inhibition of PDE 1, 3, 4 and 5 showed amelioration of PAH in studies. PDE5 inhibitors belong to the established therapies. Although specific therapeutic drugs have been developed in last decades, still there is no cure for PAH available. To date, knowledge about the possible influence of newly discovered families of PDE (PDE 7-11) on PAH is poor. Up to now, PDE10 has mostly been investigated in neuronal diseases with promising results. In the field of PAH, PDE 10 is almost unknown. Interestingly, PDE 10 was reported to be increased in pulmonary arteries of monocrotaline induced hypertension in rat.

The aim of this study was to investigate if PDE 10 is a possible treatment target for PAH. For this investigation, the effect of PDE 10 on human smooth muscle cells was characterized. Smooth muscle cells of patients with idiopathic pulmonary hypertension were reported to be hyperproliferative when compared to cells of healthy individuals. The new, selective PDE10-inhibitor, PF 3188212, stopped hyperproliferation in these cells. On the molecular level, inhibition of PDE10 leads to the activation of the cAMP/protein kinase A/cAMP-response element-binding protein axis. Another factor that is influenced by PDE 10 is cyclin D1. This cell cycle protein is required for progression through the G1-Phase of the cell cycle and therefore promotes cell proliferation. The PDE10-inhibitor PF-3188212 reduced levels of cyclin D1 significantly. The effects of PDE10 inhibition were not only seen on molecular level but also in an animal model. In the monocrotaline-rat model, treatment with PDE10 inhibitor PF-3188212 showed an improved right ventricular systolic pressure, an increased cardiac index, a reduced right heart hypertrophy, and, as an indicator for reduced right heart insufficiency, an improved tricuspid annular plane systolic excursion. Histological, reduced muscularization and medial wall thickness were documented.

Taken together, all findings indicate a crucial role for PDE 10 in promoting and sustaining PAH. PF-3188212 is shown to be a potent PDE10 inhibitor.

ZUSAMMENFASSUNG

ZUSAMMENFASSUNG

Die pulmonal arterielle Hypertonie (PAH) ist eine progressive Erkrankung der Lunge, die durch Kontraktion und Remodeling den Widerstand der Arterien und somit den Blutdruck im Lungenkreislauf erhöhen. Die Genese dieser Erkrankung wird durch viele Mediatoren, hoch oder herunterreguliert, begünstigt. Die second messenger zyklisches Adenosinmonophosphat (cAMP) und zyklisches Guanosinmonophosphat (cGMP) werden als zwei der vielen Mediatoren angesehen. In experimentellen Studien und in Patienten mit PAH zeigten sich die zyklischen Nukleotide erniedrigt. Der Abbau von cAMP und cGMP wird durch Phosphodiesterasen (PDE) reguliert. Durch die Reduktion des Vorkommens der second messenger begünstigen PDE die PAH. Die Hemmung der PDE 1, 3, 4 und 5 zeigte in Studien die Erhöhung der zyklischen Nukleotide und eine Linderung der PAH. PDE5-Inhibitoren gehören zu den etablierten spezifischen Therapeutika. Obwohl in den letzten Jahrzehnten einige spezifische Medikamente entwickelt wurden, fand sich bisher keine Therapie zur Heilung der Krankheit. Über den möglichen Einfluss der neu entdeckten Familien der PDE (PDE7-11) in der PAH ist bisher wenig bekannt. Bisherige Studien wurden vor allem im Zusammenhang mit neurologischen Erkrankungen gemacht, mit guten Erfolgen. PDE10 ist bisher weitgehend unbekannt im Gebiet der PAH. Interessanterweise ist PDE10 in den Pulmonalarterien von Ratten mit Monocrotalin-induzierter PAH erhöht.

Ziel dieser Studie war es, PDE 10 als möglichen Therapieansatz in der PAH zu prüfen. Hierzu wurde die Wirkung von PDE10 auf humane glatte Muskelzellen genauer charakterisiert. Glatte Muskelzellen von Patienten mit idiopathischer pulmonal-arterieller Hypertonie zeigten sich im Vergleich zu Zellen von gesunden Individuen proliferativer. Dieser Effekt konnte mittels Hemmung durch den neuen PDE10-Inhibitor PF-3188212 gestoppt werden. Auf zellmolekularer Ebene wird bei der Hemmung von PDE10 die cAMP/Proteinkinase A/cAMP-response element-binding protein-Axe aktiviert. Ein weiterer Faktor, der durch den PDE10-Inhibitor beeinflusst wird, ist Cyclin D1. Dieses Zellzyklusprotein vermittelt den Übergang in die G1-Phase und fördert somit die Zellproliferation. Der PDE10-Inhibitor konnte Cyclin D1 signifikant reduzieren. Der Effekt der PDE10-Hemmung ließ sich nicht nur auf molekularer Ebene, sondern auch im Tierexperiment zeigen. Bei mit Monocrotalin behandelten Ratten, zeigte sich nach Behandlung mit dem PDE10-Inhibitor PF-3188212 ein verbesserter rechts ventrikulärer systolischer Druck, ein erhöhter Herzindex, eine verminderte Rechtsherzhypertrophie und als Maß der verminderten Rechtsherzbelastung eine erhöhte systolische Exkursion

ZUSAMMENFASSUNG

der Triksupidalklappenebene. Histologisch fand sich ein erniedrigter Grad der Muskularisierung und der medialen Wanddicke.

Zusammengefasst belegen alle Erkenntnisse die einflussreiche Rolle von PDE 10 in der Förderung und Aufrechterhaltung der PAH. PF-3188212 stellt sich als wirkungsvoller PDE10-Inhibitor dar.

1 Introduction

1.1 Pulmonary hypertension

Pulmonary Hypertension (PH) is a progressive disease with an elevated pulmonary vascular pressure. Multiple mechanisms can cause increased resistance in lung vasculature leading to PH. Independent from its genesis, augmented pulmonary vascular pressure elevates afterload in the right ventricle. With disease progression, right heart hypertrophy and right heart failure develops¹ which, if untreated, this can lead to death². PH is a disease with varying prevalence among the different groups of underlying causes^{3,4}. Severity of disease and therapeutic strategy depends on the genesis of PH⁵; however, currently no cure is available for any form of PH.

1.1.1 Definition and diagnosis of pulmonary hypertension

In 1891 the German physician Ernst von Romberg⁶ first described pulmonary vascular lesions in autopsy. Thanks to the invention of the right heart catheter (RHC), the first clinical and hemodynamic study was performed in 1951. At this time, PH was defined as a mean pulmonary arterial pressure (PAP) ≥ 25 mmHg⁷ and now is defined as a PAP ≥ 20 mmHg⁸. PH further is subclassified as isolated post-capillary PH when pulmonary vascular resistance (PVR) is < 3 Wood Units and as isolated pre-capillary PH or combined pre- and post-capillary PH when PVR ≥ 3 Wood Units. Combined pre- and post-capillary PH is given if pulmonary arterial wedge pressure ≥ 15 mmHg⁸. Normal mean PAP is around $14,0 \pm 3.3$ mmHg⁹. Assessment of mean PAP at exercise is not considered as reliable^{9,10}. Despite technological progress, the average time of diagnosis after onset of symptoms takes over two years¹¹. The long period is due to a lack of early symptoms and to their non-specificity. Initially, patients might report fatigue, dyspnea, angina and syncope^{5,12}. Additional detected arterial hypoxia and PH associated diseases like left heart disease, chronic pulmonary disease or infections should lead to further examination¹². Probability of PH must be determined by echocardiography¹³. If PH is diagnosed by RHC and valvular disease is ruled out, the next step is to classify the subgroup by high-resolution computed tomography or ventilation/perfusion lung scan^{10,14}.

1.1.2 Classification of pulmonary hypertension

The classification of PH evolved over six World Symposiums on PH. The original

INTRODUCTION

classification from 1973 consisted of the two groups: 1) primary pulmonary hypertension and 2) secondary pulmonary hypertension to distinguish PH with or without known causes^{2,15}. The progress of understanding pathology, hemodynamic and therapeutic approaches helped to define five groups with similar parameters (Second World Symposium on PH). The current classification (Table 1) was made on the sixth World Symposium in Nice, France in 2018⁸. It now serves as a tool for clinicians not only to categorize PH but also to find the best available treatment.

Table 1: Updated clinical classification of PH (updated from Nice, 2018)⁸

1. Pulmonary arterial hypertension (PAH)
1.1 Idiopathic PAH 1.2 Heritable PAH 1.3 Drug- and toxin-induced PAH 1.4 PAH associated with 1.4.1 Connective tissue disease 1.4.2 HIV infection 1.4.3 Portal hypertension 1.4.4 Congenital heart disease 1.4.5 Schistosomiasis 1.5 PAH long-term responders to calcium channel blockers 1.6 PAH with overt features of venous/capillaries (PVOD/PCH) involvement 1.7 Persistent PH of the newborn syndrome
2. Pulmonary hypertension due to left heart disease
2.1 PH due to heart failure with preserved left ventricular ejection fraction 2.2 PH due to heart failure with reduced left ventricular ejection fraction 2.3 Valvular heart disease 2.4 Congenital/acquired cardiovascular conditions leading to post-capillary PH
3. Pulmonary hypertension due to lung diseases and/or hypoxia
3.1 Obstructive lung disease 3.2 Restrictive lung disease 3.3 Other lung disease with mixed restrictive/obstructive pattern 3.4 Hypoxia without lung disease 3.5 Developmental lung disorders
4. PH due to pulmonary artery obstructions
4.1 Chronic thromboembolic pulmonary hypertension 4.2 Other pulmonary artery obstructions 4.2.1 Sarcoma (high or intermediate grade) or angiosarcoma 4.2.2 Other malignant tumors: Renal carcinoma, Uterine carcinoma, Germ cell tumors of the testis, Other tumors 4.2.3 Non-malignant tumors: Uterine leiomyoma 4.2.4 Arteritis without connective tissue disease 4.2.5 Congenital pulmonary artery stenoses 4.2.6 Parasites: Hydatidosis
5. Pulmonary hypertension with unclear and/or multifactorial mechanisms
5.1 Hematologic disorders: chronic hemolytic anemia, myeloproliferative disorders 5.2 Systemic and metabolic disorders: pulmonary Langerhans cell histiocytosis, Gaucher disease glycogen storage disease, neurofibromatosis, sarcoidosis 5.3 Others: chronic renal failure with or without hemodialysis, fibrosing mediastinitis 5.4 Complex congenital heart disease

PAH: pulmonary arterial hypertension; PVOD: pulmonary veno-occlusive disease;
PCH: pulmonary capillary haemangiomas

1.2 Pulmonary arterial hypertension

PH due to left heart disease is the clinically most relevant group⁵ of PH. In the retrospective Armadale echocardiography study, prevalence of group 2 was 250/100000 habitants while prevalence of group 1 was 15/100000 habitants¹⁶. In a French and Scottish register, the prevalence of pulmonary arterial hypertension (PAH) ranged from 15-52 patients per million^{3,17}. Despite being a rare disease, for affected persons PAH is a fatal diagnosis. The subgroup idiopathic PAH often affects middle-aged women³ and, untreated, has a poor prognosis with a mean survival of 2.8 years². Other subgroups in PAH are classified as heritable or due to drugs, toxins or infections¹⁸.

There are several therapeutic options to decelerate the progress of the disease¹⁹⁻²¹. Currently, there is no cure available. And even with specific drug therapy, the prognosis is still poor with a median survival time of just over 7 years²². Although our knowledge of the genesis of PAH has increased in the last decades, the pathobiology of PAH still is to be illuminated.

1.2.1 Pathogenesis and molecular mechanisms

As PAH is a heterogeneous group, there are several known risk factors that promote its pathogenesis. Heritable factors, diverse drugs and toxins, hypoxia as well as multiple PAH associated diseases like connective tissue disease and HIV infection or a combination of these factors contribute to PAH²³. Injury might partially initiate the disease²⁴. Involved in pathogenesis are endothelial cells, smooth muscle cells (SMC), fibroblasts and adventitia^{25,26}. Four mechanisms are responsible for increased pulmonary vascular pressure: 1) the imbalance of vasoactive mediators leads to dysregulation of vascular tone^{27,28}, 2) endothelial dysfunction results in vasomotion and remodeling²⁵, 3) a hypercoagulable phenotype²⁹ causes *in situ* thrombosis and 4) inflammation thickens adventitial layer¹⁴.

Previously, vasoconstriction was believed to be a major cause of disease. Vasoconstriction is mainly caused by endothelial dysfunction. The secretion of vasodilators like NO²⁸ and prostacyclin³⁰ is depleted in PAH patients. On the other hand, pulmonary endothelial cells release high levels of vasoconstrictive mediators such as endothelin²⁷ and thromboxane³¹. These mediators not only contribute to vasoconstriction but also exert a proliferative effect on SMC^{25,32}. Nowadays, the great impact of proliferation to the genesis of disease is known³³. Many growth factors such as platelet derived growth factor (PDGF)³⁴ contribute to proliferation. Consequent imbalance of proliferation and apoptosis is designated as pulmonary vascular remodeling (Figure 1)

INTRODUCTION

and results in structural change in pulmonary vascular bed³³. In addition to proliferation, pulmonary vascular remodeling comprises hypertrophy of vascular cells and recruitment of fibroblasts, pericytes and monocytes²⁶.

Recent investigations report that inflammation also plays a role in the genesis of PH²⁴. The precise role of inflammatory mediators like IL-1 (interleukin 1), IL-6 (interleukin 6) and TGF (transforming growth factor) is still not clear³⁵. Cytokines might be part of a healing process, but at least their proliferative effects contribute to the pathogenesis of PAH³⁶.

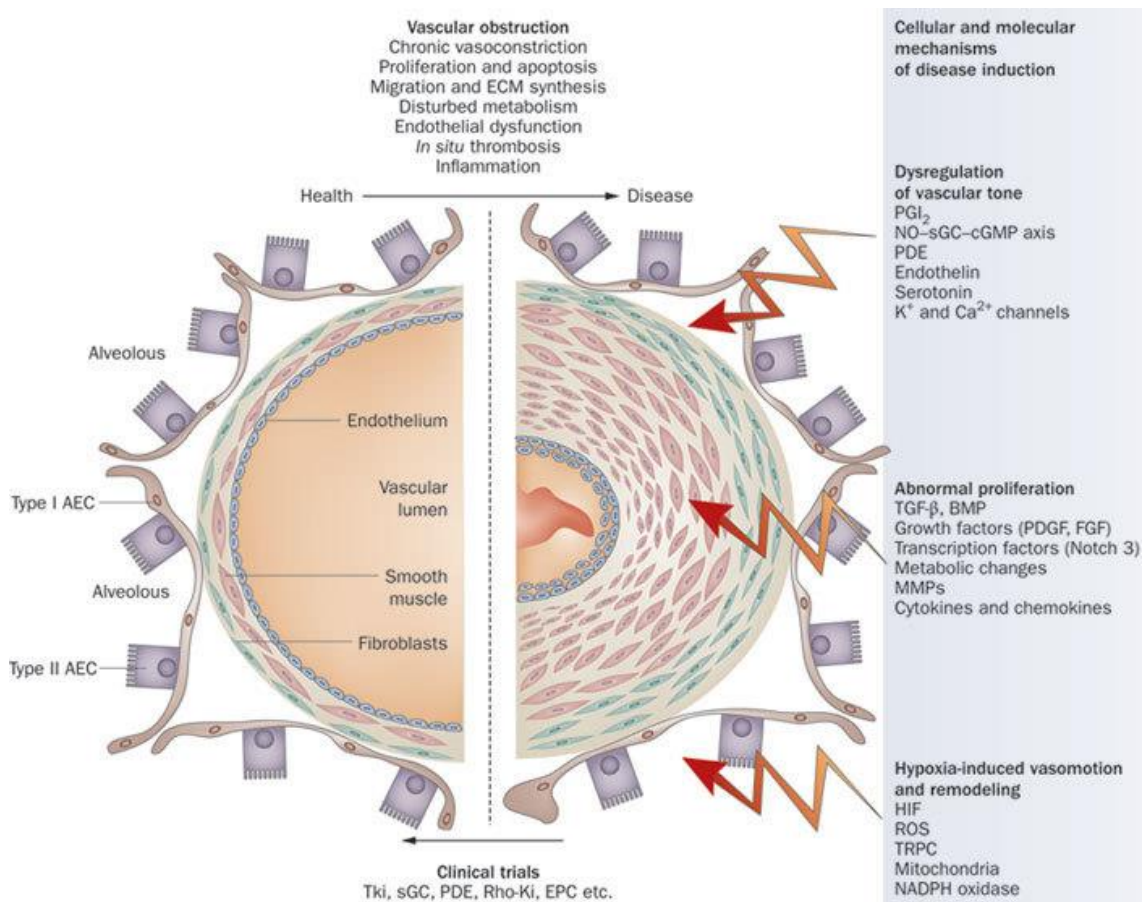


Figure 1: Vascular remodeling in pulmonary arterial hypertension. Putative therapeutic targets are indicated. Abbreviations: 5-HT, 5-hydroxytryptamin; K- and Ca-channels, potassium and calcium channels; AEC, alveolar epithelial cells; BMP, bone morphogenetic protein; cGMP, cyclic guanosine monophosphate; ECM, extracellular matrix; EGF, epidermal growth factor; EPC, endothelial progenitor cells; FGF, fibroblast growth factor; HIF, hypoxia inducible factor; MMPs, matrix metalloproteinases; NADPH, nicotinamide adenine dinucleotide phosphate; NO, nitric oxide; PDE, phosphodiesterase; PDGF, platelet-derived growth factor; PGI₂, prostaglandin I₂; Rho-kinases; ROS, reactive oxygen species; sGC, soluble guanylate cyclase; TGF-β, transforming growth factor-β; TK, tyrosine kinase; TKi, tyrosine kinase inhibitor; TRPC, transient receptor potential cation channels; VEGF, vascular endothelial growth factor. (Schermuly, R.T., 2011)³³.

Vascular remodeling as well as vasoconstriction, *in situ* thrombosis and inflammation are

INTRODUCTION

influenced by numerous mediators³³. Alterations in the levels of nitric oxide^{28,37}, endothelin-1²⁷, prostacyclin³⁰, serotonin³⁸ and depleted function of potassium channels³⁹ observed in PAH suggest that they play key roles in the induction of PAH, even if the exact mechanisms are currently not known.

1.2.1.1 Nitric oxide pathways

Nitric oxide (NO) is a vasodilator and an inhibitor of SMC proliferation. It is synthesized primarily by endothelial NO synthase from the amino acid L-arginine. NO increases the second messenger, cyclic guanylyl monophosphate (cGMP), by stimulating soluble guanylate cyclase. cGMP activates protein kinase G (PKG) and decreases intracellular calcium levels, resulting in vasodilation. Phosphodiesterases degrade cGMP to guanosine monophosphate (GMP) and counteract vasodilation.

High arginase levels³⁷ as well as reduced expression of NO synthase²⁸ are implicated in the reduced NO levels observed in patients with PAH. The importance of the NO axis on the pathogenesis of PAH is also demonstrated by endothelial NO synthase-null mice. These mice are more likely to develop PAH than wild-type mice⁴⁰.

1.2.1.2 Endothelin-1

Endothelin-1(ET-1) is the most potent vasoconstrictor⁴¹. It is mainly produced by endothelial cells. ET-1, like the two isopeptides (ET-2 and ET-3), acts on two receptors. Endothelin receptor A (ETA) is mainly located in SMC while endothelin receptor B (ETB) is presented by SMC and endothelial cells. The ET-1 stimulated G-protein-coupled receptor in SMCs activates phospholipase C. Then increased intracellular calcium levels induce vasoconstriction. In addition, protein kinase C is activated. Increased ET-1 levels in PAH patients²⁷ contribute to the disease by elevated vascular tone and also by increased proliferation mediated by protein kinase C. Recent investigations suggest that ET-1 itself does not have any mitogenic effects, but in combination with other mitogens, increases human pulmonary arterial SMC (hPASMC) proliferation³². In contrast to its vasoconstrictive and mitogenic effects, ET-1 acts vasodilatory and anti-proliferatively by stimulating endothelial ETB. Stimulated endothelial cells release NO and prostacycline⁴² and reduce circulating ET-1⁴³. Although the role of ET-1 in PAH is still not clear, the correlation of ET-1 levels and severity of the disease supports the importance of ET-1 in the disease⁴⁴.

1.2.1.3 Prostacyclin and thromboxane

Prostacyclin is an arachidonic acid metabolite mainly produced by endothelial cells. It is

INTRODUCTION

a vasodilator and, in addition, inhibits platelet aggregation and SMC proliferation⁴⁵. Reduced levels of prostacyclin synthase in endothelial cells³⁰ and lower levels of prostacyclin metabolite³¹ are detected in PAH patients. Thromboxane A2 is increased in PAH patients³¹ and contributes to increased vascular pressure with its opposing effects via vasoconstriction, platelet aggregation and proliferation.

1.2.1.4 Serotonin

Serotonin (5-hydroxytryptamin, 5-HT) promotes SMC proliferation²⁵ and vasoconstriction⁴⁶. Normally, plasma 5-HT level is low thanks to uptake and storage in platelets. Plasma serotonin is elevated in patients with PAH³⁸ and serotonin uptake in platelets is decreased in 5-HT transporter knockout mice⁴⁷. SMC hyperplasia is mediated via endothelial cells and can be prevented with the 5-HT transporter inhibitor, Fluoxetine²⁵. Further, treatment with serotonin transporter inhibitors or deficiency for 5-HT transporter is protective against pulmonary vascular remodeling in mice⁴⁷.

1.2.1.5 Potassium channels

Voltage gated potassium channels have a membrane stabilizing function. In idiopathic pulmonary arterial hypertension (IPAH) patients K-channels are depleted³⁹ and lead, via calcium influx and increased intracellular calcium levels, to vasoconstriction. Dysfunctional potassium channels also enhance SMC proliferation⁴⁸.

1.2.2 Histopathology of pulmonary arterial hypertension

The cellular and molecular mechanisms contributing to PAH lead to common histological features of the disease. These abnormalities comprise all layers of the vessel walls: intima, media and adventitia²⁶. There are five characteristic structural changes of vessels and the surrounding tissue: 1) muscularization of the peripheral arteries, 2) medial hypertrophy of muscular arteries, 3) loss of small precapillary arteries, 4) neointima formation and 5) plexiform lesion formation (Figure 2)^{33,49}.

INTRODUCTION

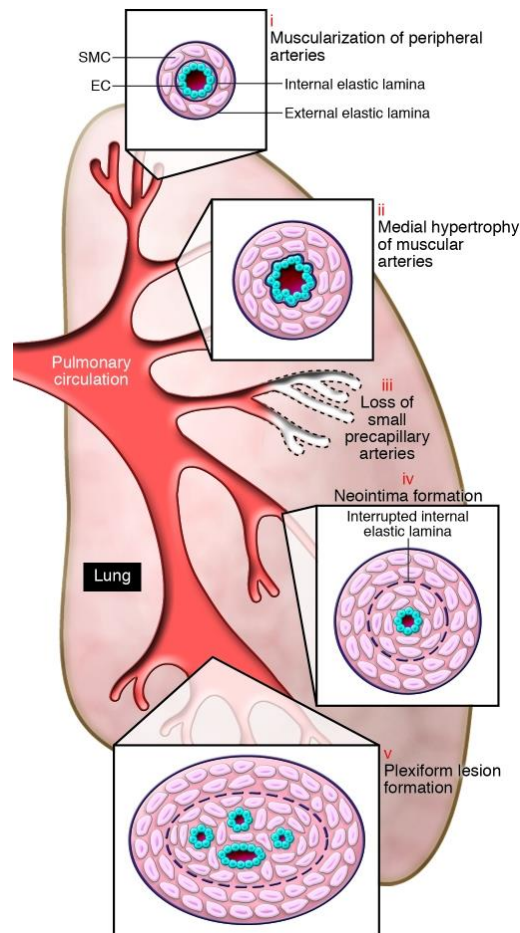


Figure 2: Pathobiology of PAH. Illustrating Schema of the different vascular abnormalities in pulmonary circulation associated with PH (Rabinovitch, M., 2008)⁴⁹.

Plexiform lesions are highly characteristic of the histopathology of PAH. In these lesions, vascular diameter is obstructed by channels covered by endothelial cells and surrounded by SMCs, myofibroblast cells and mononuclear cells⁵⁰. Proliferating endothelial cells can also interrupt internal elastic lamina which is designated as neointima formation. These cells, as well as proliferating SMCs contribute to vascular remodeling^{51,52}. Peripheral muscularization of small vessels is also reported. In vessels of 20-100 μ m diameter, a medial hypertrophy is noted. In contrast to proliferation, there is also a loss of precapillary arteries. All abnormalities, especially those caused by proliferation, contribute to a narrowing of the vessel wall¹¹.

INTRODUCTION

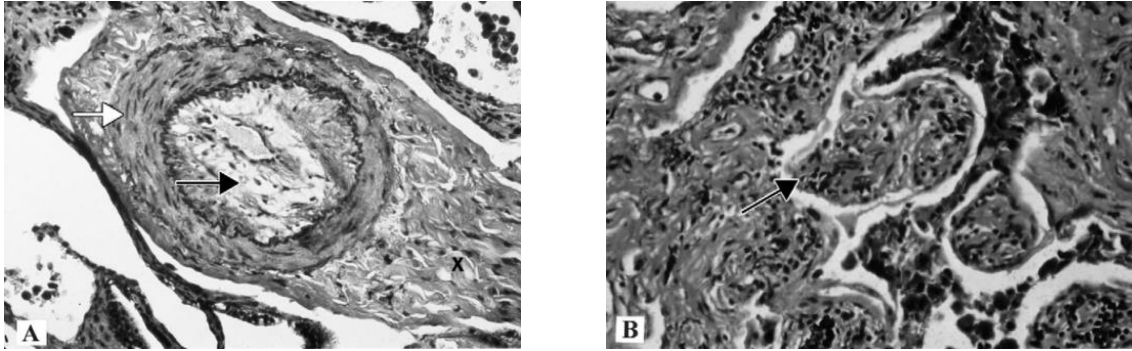


Figure 3: Histology of PAH. **A:** Muscular pulmonary artery from a PPH patient with medial hypertrophy (white arrow), luminal narrowing by intimal proliferation (black arrow), and proliferation of adventitia (X). **B:** Characteristic plexiform lesion from an obstructed muscular pulmonary artery (arrow). (Gaine, S.P. and Rubin, L.J., 1998)¹¹

Consequently, axial diameter is decreased and pressure is elevated in lung vessels. As result, the right heart adapts to maintain blood flow¹.

1.2.2.1 Hemodynamics and right heart function in pulmonary arterial hypertension

The elevated pulmonary pressure in PAH results in augmented afterload for the right ventricle. More strength is needed to provide the left ventricle with an equal volume of blood. The right ventricle is forced to hypertrophy¹. This alteration can be pictured as right heart hypertrophy by echocardiography¹³. A more commonly used parameter to diagnose right heart failure than increased right ventricular mass is systolic PAP measured by echocardiography. Pulmonary arterial systolic pressure (PASP) is estimated by the simplified Bernoulli equation with tricuspid regurgitation velocity and right atrial pressure. Other signs for PH in echocardiography can be a change of right ventricular anatomy, alteration of right ventricular outflow and increased diameter of inferior vena cava and increased area of right atrium¹³. If the probability of PH is high, RHC can be performed for diagnosis⁵. A mean PAP > 20 mmHg confirms PH⁷.

Right heart failure is the limiting factor in PH and untreated, causes death². In RHC, pulmonary wedge pressure can be measured for further classification of PH subgroup to initialize adequate treatment and to prevent right heart failure⁵. For PAH, wedge pressure is < 15 mmHg⁵.

1.2.3 Treatment of pulmonary arterial hypertension

Pharmaceutical therapy consists of supportive therapy comprising oral anticoagulants, diuretics, oxygen and digoxin. In addition, a specific therapy is needed to improve the

INTRODUCTION

patient's life, to minimize the risk of complications and to prolong time until death. If calcium antagonists are not effective⁵³⁻⁵⁵, there are basically three main pathways for medical targets: the NO pathway⁵⁶⁻⁵⁸, endothelin^{59,60} and the prostacyclin^{61,62} pathway. To reduce side effects and to reach the best possible results by additive treatment effects, a combination of medications acting on different pathways is believed to be the best concept²³. Shown below are the specific medications proposed in the *ESC/ERS guidelines for the diagnosis and treatment of pulmonary hypertension* from 2015⁵.

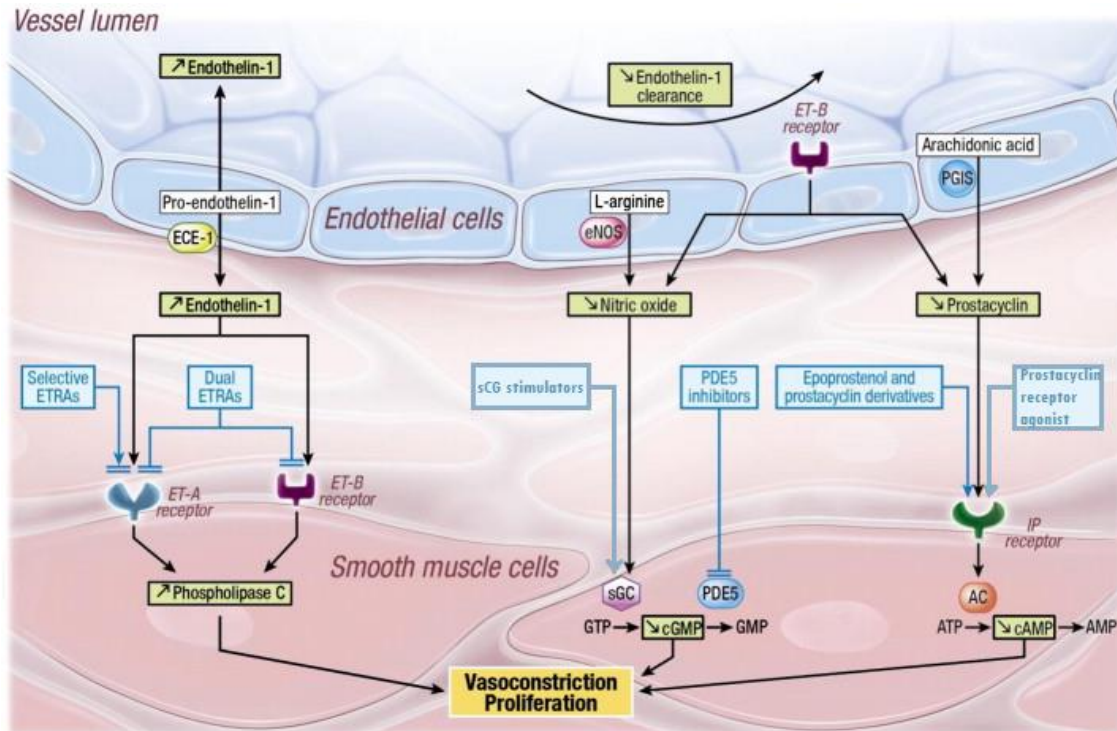


Figure 4: Endothelial dysfunction in pulmonary arterial hypertension and current therapeutic target therapies. Blue boxes show current therapies (Modified from Montani, D., 2014)⁶³.

1.2.3.1 Calcium channel blockers

Calcium channel blockers lower intracellular calcium levels and thus act as vasodilators. Evidence of treatment with calcium antagonists like nifedipine, diltiazem and amlodipine in PAH is very limited⁶⁴. Only a few single center studies show improved hemodynamics and survival rate of calcium channel blockers on so called “responders”^{53,55}. As longtime benefit is limited to a small number of IPAH patients (estimated to be approximately 6.8%), and because side effects such as peripheral edema and hypotension can occur⁵⁵, treatment is restricted to patients with acute vasoreactivity, and safety as well as efficacy have to be controlled⁶⁵.

INTRODUCTION

1.2.3.2 Prostanoids

Continuous intravenous epoprostenol was the first specific therapy for PAH. Vasodilation, reduced platelet aggregation and proliferation ameliorate symptoms⁴⁵. Epoprostenol treatment results in improved exercise capacity, better hemodynamics and shows increased survival⁶¹. Due to the short half-life of the synthetic prostacyclin epoprostenol (3-5min) and the need for continuous i.v. application, further analogues have been developed. Iloprost, treprostinil and beraprost can be applied orally, i.v. or by inhalation. Treatment results show variable efficacy. All prostanoids and analogues have similar side effects such as diarrhea, flushing and headaches^{4,66,67}. The first oral, selective Prostacyclin-IP-receptor agonist, selexipag, is now available⁶². It showed a reduction of clinical worsening and adverse events in a randomized controlled trial¹⁹.

1.2.3.3 Endothelin-1 antagonists

ET-1 causes vasoconstriction and pulmonary arterial smooth muscle cell (PASMC) proliferation via two receptor types (ETA and ETB). Endothelin receptor antagonists (ERA) are either dual inhibitors, acting on both receptors, or selective inhibitors for ETA. Ambrisentan is a non-sulfonamide, propanoic acid-based A-selective ERA. Bosentan is a synthetic dual ERA. Both showed improvement in exercise capacity, WHO functional class and time to clinical worsening in randomized controlled trials^{59,68}. Mild to moderate side effects like peripheral edema, headache, nasal congestion and decreased hemoglobin concentration have been reported⁶⁹. For bosentan, a dose-dependent hepatic toxicity was described in the BREATHE-1 study⁶⁰. The long-term randomized controlled trial SERAPHIN documented significantly reduced combined primary endpoint morbidity and mortality in PAH patients receiving the dual ERA macitentan. While liver enzyme levels did not differ, reduction in blood hemoglobin, increased headache and nasopharyngitis was observed more often in the macitentan group compared to the placebo group²⁰.

1.2.3.4 Nitric oxide pathway

Phosphodiesterase (PDE) type 5 is mainly abundant in lung tissue and degrades cGMP⁷⁰. PDE 5 inhibition results in increased intracellular cGMP concentration and vasodilation. PDE 5 inhibitors also have antiproliferative effects on hPASMCs⁷¹. Currently there are three PDE 5 inhibitors available: Sildenafil, tadalafil and vardenafil. They all show improvement on exercise capacity, hemodynamics and time to clinical worsening in randomized controlled trials⁵⁶⁻⁵⁸. In these studies, mild to moderate side effects related to vasodilation such as headache, flushing and epistaxis are noted for

INTRODUCTION

each PDE 5 inhibitor.

The soluble guanylate cyclase (sGC) stimulator riociguat increases cGMP levels like PDE 5 inhibitors. In contrast to PDE 5 inhibitors it does not stop the degradation of cGMP but enhances cGMP synthesis by acting in synergy with NO and by directly stimulating sGC⁷². These mechanisms make riociguat independent from endogenous NO production, which can be depleted in PAH patients^{28,37}. In the PATENT study, exercise capacity, hemodynamics and time to clinical worsening was improved by oral riociguat treatment²¹. Reported adverse effects such as syncope and dizziness are presumably caused by low blood pressure⁷³. Because of the synergistic effect on hypotension, riociguat and PDE inhibitors must not be combined⁷⁴, whereas a combination of riociguat with medications from other treatment branches ameliorates symptoms²¹.

1.2.3.5 Current Investigations

Investigations on tyrosine kinase inhibitors, inhaled vasointestinal peptide and serotonin antagonists as future treatments failed. Yet promising new targets like rho kinase inhibitor, vascular endothelial growth factor receptor antagonists, angiopoietin-1 inhibitor and elastase inhibitor are in early stages of study.

1.3 Phosphodiesterase

1.3.1 Cyclic nucleotides

The cyclic nucleotides adenosine 3', 5' cyclic monophosphate (cAMP) and guanosine 3', 5' cyclic monophosphate (cGMP) act as so called second messengers. They transmit primary extracellular signals to achieve an intracellular response by activating downstream targets⁷⁵. This mechanism regulates various functions depending on cell and tissue type. In the case of pulmonary smooth muscle cells, vascular tone and proliferation^{71,76} are controlled.

INTRODUCTION

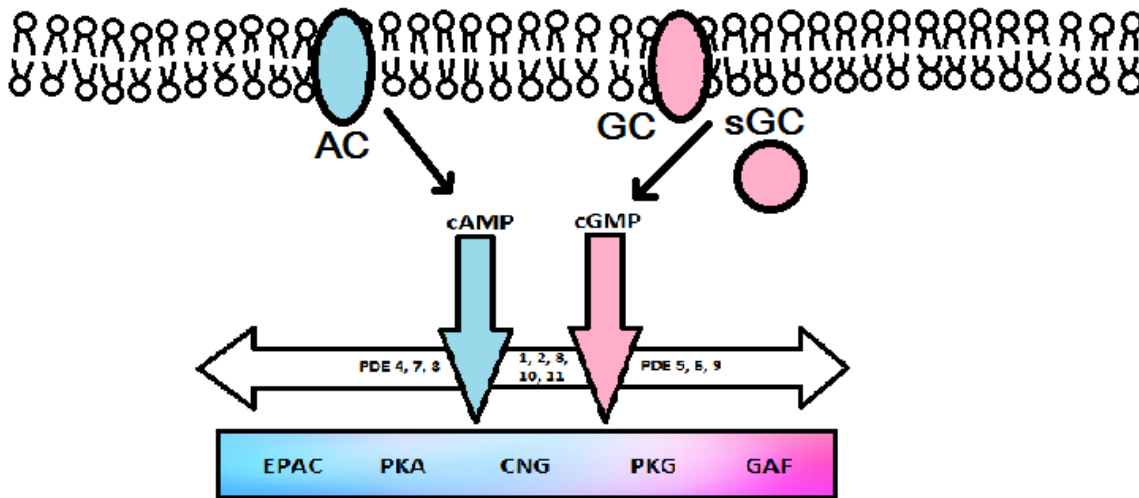


Figure 5: Cyclic nucleotides signaling pathway. AC, receptor linked adenylyl cyclase, and GC, guanylyl cyclase, as well as sGC, soluble guanylyl cyclase, enhance synthesis of cAMP, and cGMP, respectively. Cyclic nucleotides stimulate EPAC, exchange protein directly activated by cAMP; PKA, protein kinase A; CNG, cyclic nucleotide-gated channel; PKG, protein kinase G; GAF domains. Degradation is mainly regulated by PDE isoforms. Depending on the isoform either cAMP or cGMP or both are degraded. Modified from Keravis 2012⁷⁰.

Generally, cAMP and cGMP homeostasis are maintained. When extracellular messengers bind to membrane receptors, an intracellular cascade of signal transmission proceeds. First, the receptor-linked adenylyl cyclase as well as receptor-linked and soluble guanylyl cyclases are stimulated. This increases the synthesis of cAMP and cGMP. The targets of the cyclic nucleotides are mainly protein kinase A (PKA) and protein kinase G (PKG), respectively. Activated PKA and PKG lead to multiple cellular responses. Cyclic nucleotides activate not only protein kinases but also exchange protein directly activated by cAMP (EPAC), cyclic nucleotide-gated channel (CNG), as well as PDEs itself via cGMP-specific phosphodiesterases, adenylyl cyclases, and FhIA (GAF) domains⁷⁰ (Figure 5).

Once synthesized, the duration and localization of the increased amount of cyclic nucleotides is primarily dependent on PDE activity⁷⁷. PDEs degrade cyclic nucleotides and thus the regulate cellular reactions to incoming signals^{75,77}.

1.3.2 Cyclic nucleotide phosphodiesterases

1.3.2.1 The functions of cyclic nucleotide phosphodiesterases

Phosphodiesterases (PDE) degrade cyclic AMP and GMP by catalyzing hydrolysis of the P-O3' bond to inactivate cyclic nucleotides. The products of hydrolysis are 5'-AMP and 5'-GMP, respectively⁷⁸.

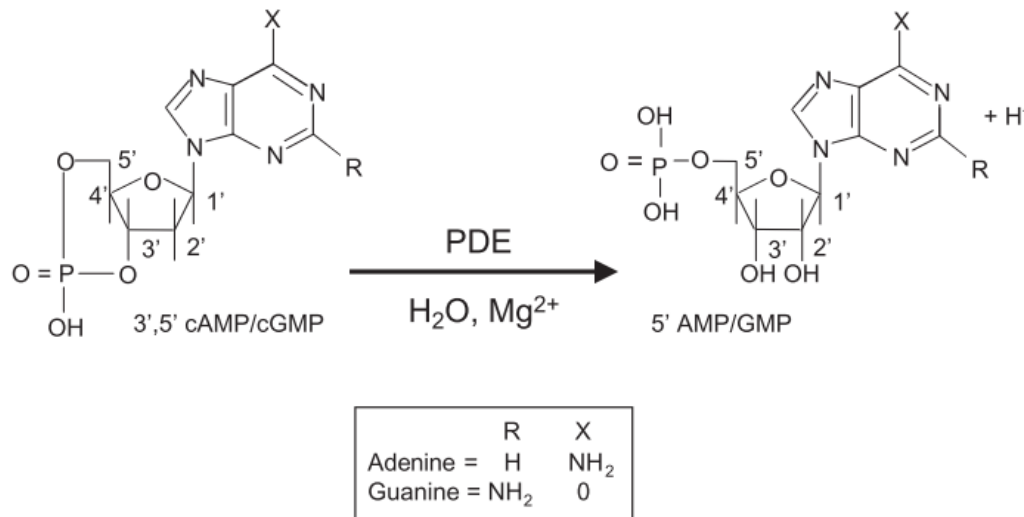


Figure 6: Cyclic nucleotide hydrolysis by cyclic nucleotide phosphodiesterase. (Lugnier, C., 2006)⁷⁸

Variant PDE isoforms with distinct substrate specificity and velocity in hydrolyzing cyclic nucleotides are distributed in cells and tissues⁷⁰. So, the duration of increased levels of cAMP and cGMP depends mainly on the characteristics of the PDE forms present. Degradation has a huge time range that lasts from milliseconds⁷⁹ to hours. Not only is this time dynamic aspect of cyclic nucleotides controlled by PDEs, but also the subcellular compartmentalization⁸⁰. Without PDEs, increased level of cyclic nucleotides would distribute randomly throughout the cell. In this case, higher levels of cyclic nucleotides would be needed to activate targets and would result in unspecific activation. PDEs also help to restrict the intracellular diffusion of cAMP and cGMP and thus effect pools of cyclic nucleotides to help ensure adequate cellular response^{80,81}. Another way that PDEs modify cyclic nucleotide signaling is via cross talk between the cAMP and cGMP pathways⁸⁰. Some PDE isoforms are targets of cGMP. PDEs can be either activated or inhibited by cGMP. Via this connection, cGMP can influence the degradation of cAMP⁸².

INTRODUCTION

1.3.2.2 Family of phosphodiesterases

PDEs are classified in 11 families, encoded by 21 genes and an abundance of isoforms^{78,83}. In nomenclature the first Arabic number indicates the family. The following letter determines the encoding gene. Last number shows the isoform⁷⁷.

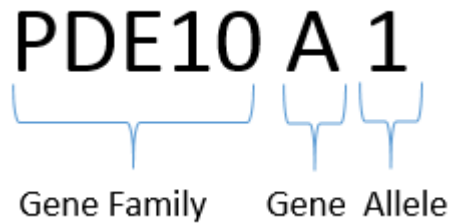


Figure 7: Nomenclature of phosphodiesterase (Adapted from Beavo, J. 1994)⁸⁴.

The first purification of PDEs was published in 1962 by Butcher and Sutherland⁸⁵. Long known PDEs are well characterized, while investigations now focus on the newly identified PDEs7-11⁷⁸. PDEs differ in substrate specificities, kinetic properties, tissue distribution and in reference to specific inhibitors⁷⁰ (Table 2).

INTRODUCTION

Table 2: Cyclic nucleotide PDE isozyme families.

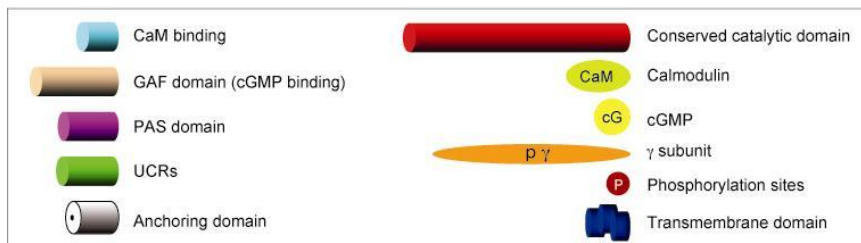
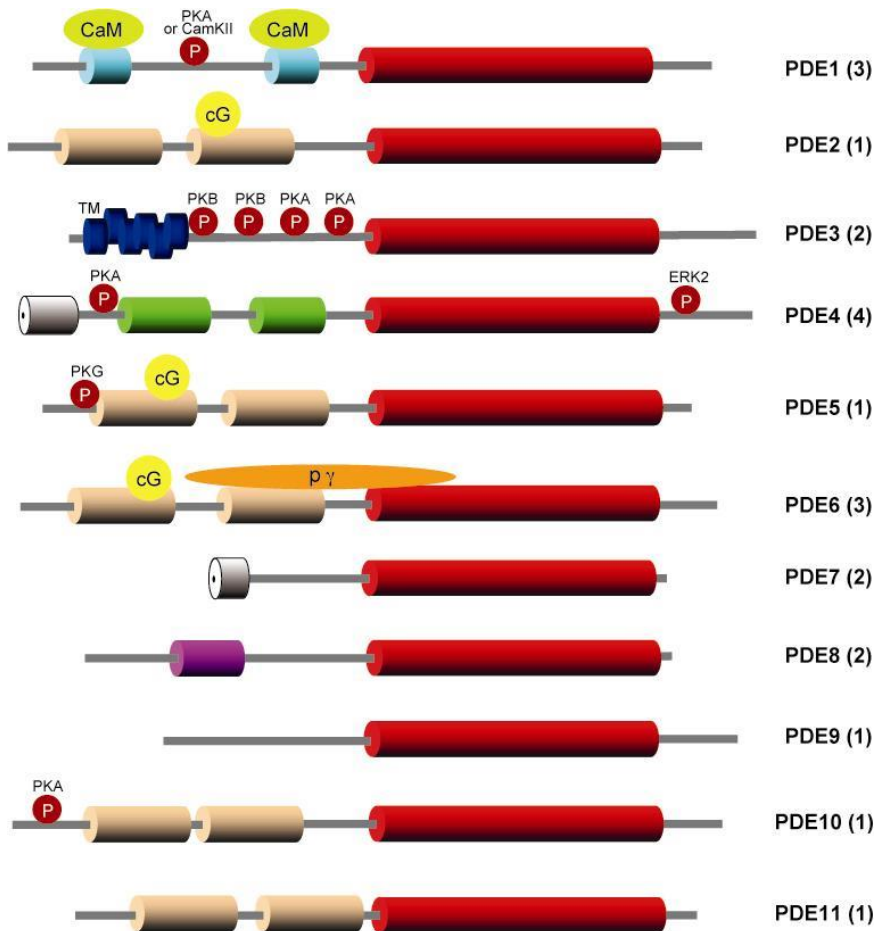
Family	Specificities	Km (μ M) cAMP/cGMP	Tissue distribution	Inhibitors
PDE1(3)	Ca ²⁺ /calmodulin-stimulated	0.3-124/0.6-6	Heart, brain, lung, smooth muscle	Nimodipine, IC86340, IC224, IC295, dioclein
PDE2(1)	cGMP-stimulated	15/15	Adrenal gland, heart, lung, liver, platelets, endothelial cells	EHNA, BAY-60-7750, PDP, IC933, oxindole, ND7001
PDE3(2)	cAMP-selective, cGMP-inhibited	0.2/0.1	Heart, smooth muscle, lung, liver, platelets, adipocytes, immunocytes	Cilostamide, milrinone, siguazodan, cilostazol
PDE4(4)	cAMP-specific, cGMP-insensitive	2/>300	Brain, Sertoli cells, kidney, liver, heart, smooth muscle, lung, endothelial cells, immunocytes	Rolipram, roflumilast, cilomast, NCS613
PDE5(1)	cGMP-specific	150/1	Lung, platelets, smooth muscle, heart, endothelial cells, brain	Zaprinast, DMPPO, sildenafil, tadalafil, vardenafil
PDE6(3)	cGMP-specific, transducing activated	2000/60	Photoreceptor, pineal gland, lung	Zaprinast, DMPPO, sildenafil, vardenafil
PDE7(2)	cAMP-specific, high-affinity rolipram-insensitive	0.2/>1000	Skeletal muscle, heart, kidney, brain, pancreas, T lymphocytes	BRL 50481, IC242, ASB16165
PDE8(2)	cAMP-selective, IBMX insensitive rolipram-insensitive	0.06/NA	Testes, eye, liver, skeletal muscle, heart, kidney, ovary brain, T lymphocytes, thyroid	PF-04957325
PDE9(1)	cGMP-specific, IBMX insensitive	NA/0.07-0.17	Kidney, liver, lung, brain	BAY-73-6691, PF-04447943
PDE10(1)	cGMP-sensitive, cAMP-selective	0.02-1/13	Testes, brain, thyroid	Papaverine, TP-10, MP-10
PDE11(1)	cGMP-sensitive, dual specificity	0.5-2/0.3-1	Skeletal muscle, prostate, pituitary gland, liver, heart	None selective

(Adapted from Keravis, T., 2012)⁷⁰

All PDE families comprise a highly conserved sequence of approximately 270 amino acids, which encodes the catalytic domain in the C-terminal region⁸⁶⁻⁸⁸. Other structural features vary between families. For example, a GAF domain is noted in families 2, 5, 6,

INTRODUCTION

10 and 11 in the N-terminus⁸⁹.



Conti M, Beavo J. 2007.
Annu. Rev. Biochem. 76:481–511

Figure 8: Structure of 11 PDE family members. Number in parenthesis gives quantity of genes (Conti M and Beavo J, 2007)⁷⁵

1.3.3 Phosphodiesterase 10 family

In 1999 PDE10 was first described in human^{90,91} and mouse⁹². The highest localization was found in brain, testes and thyroid⁹⁰. Lately, PDE10A has been considered to play a role in PH, due to the observed upregulation of PDE10A in the pulmonary vasculature of

INTRODUCTION

monocrotaline (MCT) treated rats and PAH patients⁹³.

To date, only one isoform of PDE10A, encoded by chromosome 6q26 with 779 amino acids, is known⁹⁰. The structure of PDE10A comprises the catalytic domain, two GAF domains and a phosphorylation site⁷⁵. In contrast to all other GAF domains, these are specific for cAMP instead of cGMP⁹⁴. PDE10 is a dual substrate phosphodiesterase and hydrolyzes both, cAMP and cGMP *in vitro*^{90,92}. Affinity for cAMP is higher than that for cGMP. The K_m for hydrolysis of cAMP is 0.05 μM , and the K_m for cGMP is 3 μM ⁹². The specific activity for cGMP is higher since the V_{max} ratio (cGMP/cAMP) is 4.7⁹². These kinetic characteristics explain that hydrolysis of cGMP is inhibited by cAMP. Thus, PDE10 acts as cAMP-PDE and cAMP-inhibited cGMP-PDE⁹⁰ *in vivo*. The subcellular localization of PDE10 was found in rat PASMC to be near the nucleus⁹³.

Dipyridamole, IBMX⁹⁰ and Papaverine⁹⁵, an alkaloid plant extract, are unselective PDE10 inhibitors. To maximize effects and to reduce side effects, a more specific substance is needed. To date, two selective PDE10 inhibitors are known: MP-10 and TP-10. Both have similar kinetics, such as low IC_{50} values and high selectivity⁹⁶. MP-10 and TP-10 are both being investigated as therapeutic approaches in schizophrenia⁹⁶.

1.3.4 The role of phosphodiesterase 10A in pulmonary arterial hypertension

PDEs play crucial roles in diverse signal transduction pathways. With their time dynamic regulation of cyclic nucleotides, the generation of pools of cyclic nucleotides and the ability for cross talk, they control many different functions⁷⁹⁻⁸¹. PDEs represent good therapeutic targets due to their influence on signal transduction and due to the combination of some promotive elements for effective inhibition⁹⁷. A variety of PDEs and different isoforms⁷⁸ provide the possibility for specific inhibition. Thanks to higher V_{max} at hydrolysis than at synthesis and the low levels of cyclic nucleotides, the dose of a PDE inhibitor can be quite low. Thus, PDE inhibitors belong to the established therapy regimens for a number of diseases such as heart failure, erectile dysfunction, asthma and PAH⁷⁰.

Concerning PAH, PDEs are attractive therapeutic targets regulating SMC proliferation and vasoconstriction^{71,76}. For PAH, the PDE 5 inhibitors sildenafil, tadalafil and vardenafil are clinically approved and belong to the specific therapy^{5,56-58}. In studies, the influence of other PDE families on PAH is being investigated. Expression of PDE1, PDE3, PDE5⁹⁸ and PDE10⁹³ is found to be altered in PAH patients. For the PDE families 1, 3, 4⁹⁹ and

INTRODUCTION

⁵⁷⁶ anti-proliferative effects are reported. Further, the combination of PDE 3 and 4 inhibitors¹⁰⁰ and the interaction between PDE 1 and 5 inhibitors¹⁰¹ show potential to reverse pulmonary vascular remodeling in animal models.

Since PDE10 is one of the newly identified PDE families, our knowledge about the role of PDE10 in PAH is very limited. Due to its abundance in the brain, PDE10 is mostly being investigated in neuronal diseases. It is a promising therapeutic target for Huntington's disease¹⁰², Parkinson's disease¹⁰³ and schizophrenia⁹⁶.

PDE10A might be involved in the pathogenesis of PAH. A study of Tian *et al.*⁹³ showed the specific upregulation of PDE10A in the MCT-rat model in pulmonary vasculature in comparison to peripheral vasculature. PAH in MCT rats treated with the PDE10 inhibitor papaverine is significantly ameliorated. Right heart hypertrophy decreased and hemodynamics improved. An immunocytochemical staining showed a predominance of PDE10A in the nucleus of PASMC. This finding indicates the influence of PDE10A on the cell cycle. SMC proliferation was decreased by the direct inhibitor, papaverine, as well as by specific small interfering RNAs targeting PDE10A. In this case proliferation and the cell cycle might be regulated by the downstream target, CREB.

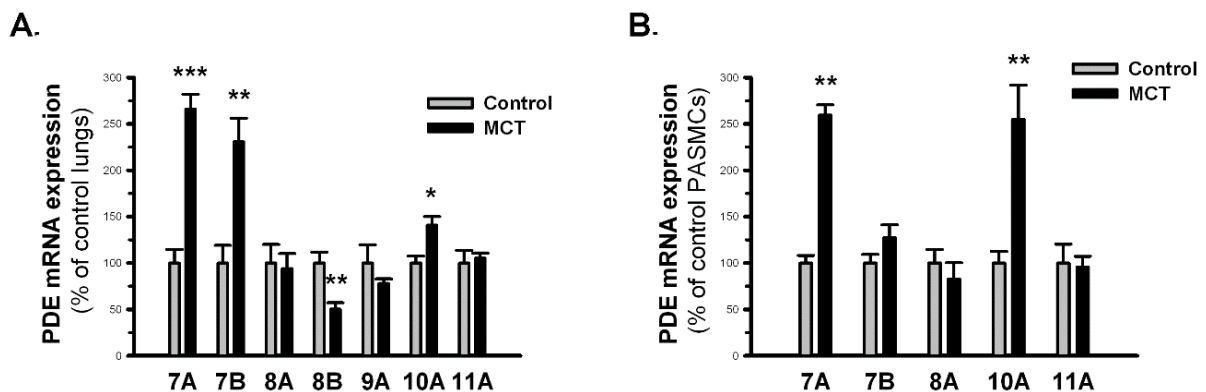


Figure 9: PDE mRNA expression in lung vasculature in rat. (From Tian *et al.*, 2011)⁹³

2 Aims of the study

Although many investigations have helped our understanding of the pathogenesis of pulmonary arterial hypertension (PAH) as well as the identification of therapeutic options, current available medical treatment is still not satisfying. Increased pulmonary vascular pressure inevitably leads to right heart insufficiency and over time, to death.

In addition to the endothelin and prostacyclin pathways, the nitric oxide pathway is the third pathway with current treatment targets for PAH. In this pathway, phosphodiesterases (PDE) influence various signal cascades in the pulmonary vasculature via cyclic nucleotides and downstream targets. By now, three inhibitors for PDE5 are used as therapy in PAH. Inhibitors for PDE 1,2,3 and 4 also show potential to ameliorate PAH in preclinical studies. Knowledge about the more recently identified PDE isoforms, PDE 7-11, in the context of PAH is poor. A previous study reported an upregulation of PDE10 in pulmonary arterial smooth muscle cells (PASMC) in rat. The aim of this study is to show the effects of PDE10 inhibition on PASMC proliferation and signaling pathways. For this work, a new PDE10 inhibitor (PF-3188212) was used.

To see, if PDE10 is not only upregulated rat but also in human PASMC a proliferation assays was performed. The proliferation of PASMC from PAH patients and donors were compared.

On the molecular level, effects PDE 10 inhibition in human PASMCs was examined by protein analysis with western blots. PDE 10 is a dual substrate PDE and can hydrolyze both cAMP and cGMP. Since affinity for cAMP is higher, focus was set on the cAMP pathway. Besides downstream products of cAMP, a variety of cell cycle proteins were of interest to see a possible influence of PDE10 in proliferation of SMC.

Animal models help to see treatment effects in preclinical studies. The monocrotaline (MCT) rat model displays structural changes in lung and heart similar to those observed in PAH patients. To see if there is a therapeutic benefit of PDE10 inhibition, MCT rats and healthy rats were treated either with a PDE10 inhibitor in two doses or placebo for three weeks. Morphologic change in lung tissue was analyzed by assessment of the degree of muscularization and of medial wall thickness. Altered hemodynamics were measured with right heart catheterization. Evaluation of right heart function was performed by echocardiography. To measure right heart hypertrophy, the mass of the

AIMS OF THE STUDY

left and right heart was noted.

3 Material and Methods

3.1 Material

3.1.1 Chemicals, reagents and kits

Product	Company
Acrylamid	Roth, Germany
Bovine serum albumin powder	Serva, Germany
Bovine serum albumin solution (2 mg/ml)	Bio-Rad, USA
D _c protein assay kit	Bio-Rad, USA
DEPC (diethylpyrocarbonate) water	Roth, Germany
Depilatory creme	Veet, Germany
DMEM	Gibco, Ireland
DMSO (dimethyl sulfoxide)	Sigma Aldrich, USA
Digest All 2 (trypsin)	Vector, USA
Enhanced chemiluminescence (ECL) kit	GE Healthcare, USA
Ethanol	SAV Liquid, Germany
Glycin	Roth, Germany
Isoflurane	Baxter Deutschland GmbH, Germany
Methanol	Sigma Aldrich, USA
Milk powder	Roth, Germany
Protein rainbow marker	Bio Rad, USA
Paraformaldehyde solution	Otto Fischar, Germany
PDE10-Inhibitor	Pfizer, USA
RNeasy mini kit	Qiagen, Netherlands
RIPA buffer	Santa Cruz, USA
RNase away	Molecular Bioproducts, USA
Saline (NaCl 0,9%)	Braun, Germany
SDS Solution 10% w/v	Promega, USA
Trichloroacetic acid	Sigma, Germany
Tris-HCl 0.5 M, pH 6.8	Amresco SOLON, USA
Tris-HCl 1.5 M, pH 8.8	Amresco SOLON, USA
Tris	Roth, Germany
Tween	Sigma, Germany

MATERIALS AND METHODS

3.1.2 Phosphodiesterase 10 inhibitor

For this study we used the newly generated compound PF-3188212 for inhibition of PDE10. It inhibits rat recombinant PDE10A enzyme assay with IC₅₀ = 0.3 nM. Selectivity for PDE10A is >1000 fold.

3.1.3 Cell culture

Smooth muscle cell basal medium	Lonza, Switzerland
Smooth muscle cell growth medium	Lonza, Switzerland
Dulbeccos Phosphate Buffered Saline	PAN Biotech, Germany
Fetal bovine serum	Biowest, Germany
Water bath for cell culture	Medingen, Germany
Water bath for tubes	HLC, Germany

3.1.4 Antibodies

Primary antibody

Antibody	Concentration	Company
GAPDH	1 : 5000	Novus biological
CREB	1 : 2000	Upstate
pCREB	1 : 2000	Upstate
PPAR γ	1 : 500	Santa Cruz
cyclin D	1 : 1000	Santa Cruz
PKA	1 : 500	Acris
pPKA	1 : 1000	Cell signaling
p21	1 : 500	Santa Cruz
p27	1 : 500	Santa Cruz

Secondary antibody

Antibody	Company
Rabbit anti-mouse IgG	Sigma-Aldrich, USA
Goat anti-rabbit IgG	Pierce, USA

MATERIALS AND METHODS

3.1.5 Equipment

Equipment	Company
Aesculap Isis GT 420	Aesculap, Germany
Anesthesia induction chamber	Vet Equip, USA
BioDoc Analyzer	Biometra, USA
Cell culture incubator, Hera Cell	Heraeus, Germany
Centrifuge 5417 R	Eppendorf, USA
Electrophoresis chamber	Bio-Rad
Freezer (+4°C,-20°C,-80°C)	Bosch, Germany
Heating Block	Grant, GB
Infinite® 200 microplate reader	Tecan, Switzerland
Inolab PH meter	WTW, Germany
Light microscope	Leica, Germany
Magnetic stirrer	Heidolph, Germany
Mikrotip BP Foundation System	AD Instruments, New Zealand
Millar Single Pressure Catheter; SPR-320	Millar, USA
Mx3000P® QPCR system machine	Agilent Technologies, USA
Spectrophotometer	NanoDrop Technologies, USA
Pipetboy and pipettes	Eppendorf, USA
Shaker	Biometra, USA
Ultrapure	Merck, Germany
Vortex mixer	Scientific Industries, USA
Water bath cell culture	Memmert, Germany
Western blot unit	Biometra, USA
Vapor 19.3	Dräger, Germany
Ultrasound Vevo 2100	Visualsonics, Canada
Vaporizer	Visualsonics, Canada

3.1.6 Other Materials

Cell culture dishes (60 and 100 mm) and plates, glass pipettes and falcon tubes were purchased from Greiner (Germany). Other material was purchased as listed below.

MATERIALS AND METHODS

AGFA cronex 5 medical X-ray film	AGFA, Belgium
Film cassette	Kodak, USA
Gel blotting paper	Whatman, USA
Supported nitrocellulose membrane	Bio-Rad, USA
Radiographic film hypersensitive	GE Healthcare, USA
Tips (10, 100, 1000µl)	Sarstedt, Germany
Cell scratcher	Sarstedt, Germany

3.2 Methods

3.2.1 Animal model

Male Sprague-Dawley rats were purchased from Charles River Laboratories, Sulzfeld, Germany. Four to five animals per cage were held at 22°C +/- 2°C room temperature with day/light cycle of 12 hours per day (relative saturation 55% +/- 10%). Nutrition consisted of Altromin standard diet and water available *ad libitum*. The weight was 300 to 350 g per rat at an age of 12 weeks. Study protocols were approved by the Federal Authorities for Animal Research of the Regierungspräsidium Giessen (Hessen, Germany; reference number GI 20/10 Nr.44/2013). Experiments were performed according to the National Institutes of Health Guidelines on the Use of Laboratory Animals in the context of the ECCPS platform for small animal phenotyping.

3.2.1.1 Monocrotaline-induced pulmonary hypertension rat model

The alkaloid monocrotaline (MCT) (Sigma Aldrich) was used to induce pulmonary hypertension. 0.375 g MCT was dissolved in 4.5 ml hydrogen chloride (HCl) and adjusted to pH 7.4 with 1 mol/L sodium hydroxide (NaOH). Rats were randomized to two groups: treated and control. Single shot subcutaneous (s.c.) injection of 60 mg per kg bodyweight in the neck was performed in MCT groups. Control rats got same volume of saline injected.

3.2.1.2 Experimental groups

Rats were distributed into two major groups: one MCT-group and one healthy-group as a control. After three weeks, the effects of MCT and saline injection on right ventricle were measured by echocardiography. Then animals in each major group were randomized into three minor groups with either application of placebo, 25 mg/kg PDE10

MATERIALS AND METHODS

inhibitor or 50 mg/kg PDE10 inhibitor. Treatment was given orally once per day. In week five, echocardiography, catheterization and organ harvest were performed.

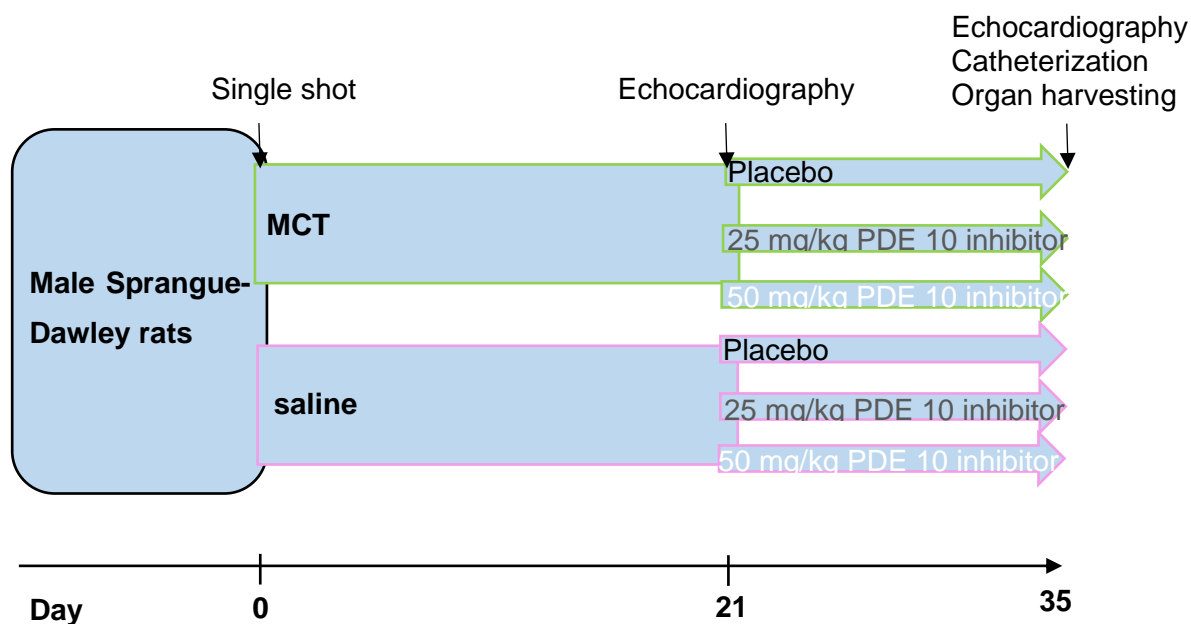


Figure 10: Study design. Rats were randomly distributed to MCT or healthy group. One time single shot injection of either MCT or Saline was performed on day 0. Treatment started at day 21 and comprised one oral dose of placebo, 25 mg/kg or 50 mg/kg PDE10 inhibitor daily. Echocardiography was performed in weeks three and five. Left heart catheterization and organ harvest followed in week 5.

3.2.1.3 Transthoracic echocardiography

Echocardiography was performed in weeks three and five as described before¹⁰⁴. Rats were placed into an anesthesia induction chamber. After induction with isoflurane (3%) at a gas flow of 2 to 3 liter/min., rats were placed in a supine position on a heating platform and anesthesia was maintained with 1.0 to 1.5% of isoflurane and 100% O₂. Chest hair was removed by shaving and chemical hair remover to improve image quality. Heart rate and temperature was monitored throughout all assessments. Prewarmed ultrasound gel was placed on the shaved chests. Transthoracic echocardiography was performed with a Vevo 2100 system and a 13- to 24-MHz transducer (MS250, rat cardiovascular, VisualSonics). To assess right ventricular function, tricuspid annular plane systolic excursion (TAPSE) and cardiac index (CI) was measured. For TAPSE, the movement of the tricuspid plane area is measured in 4-chamber view in M-mode. A cursor was placed between the tricuspid valve and right ventricular free wall (figure 11). Although it is only a two-dimensional parameter representing the function of a 3D structure, the advantage

MATERIALS AND METHODS

of this metric is the feasibility¹³.

In the parasternal short-axis view, pulmonary arterial diameter was measured in the pulmonary outflow tract during mid systole. Again, in the parasternal short-axis view, pulmonary artery velocity time integral (PA VTI) was measured by pulsed-wave doppler. Then CI was calculated by PA VTI, pulmonary arterial area, derived from PA diameter, and heart rate. CI is given as ml/min normalized to 100 g of bodyweight. Echocardiography was kindly performed by Dr. Akylbek Kojonazarov within the small animal phenotyping platform.

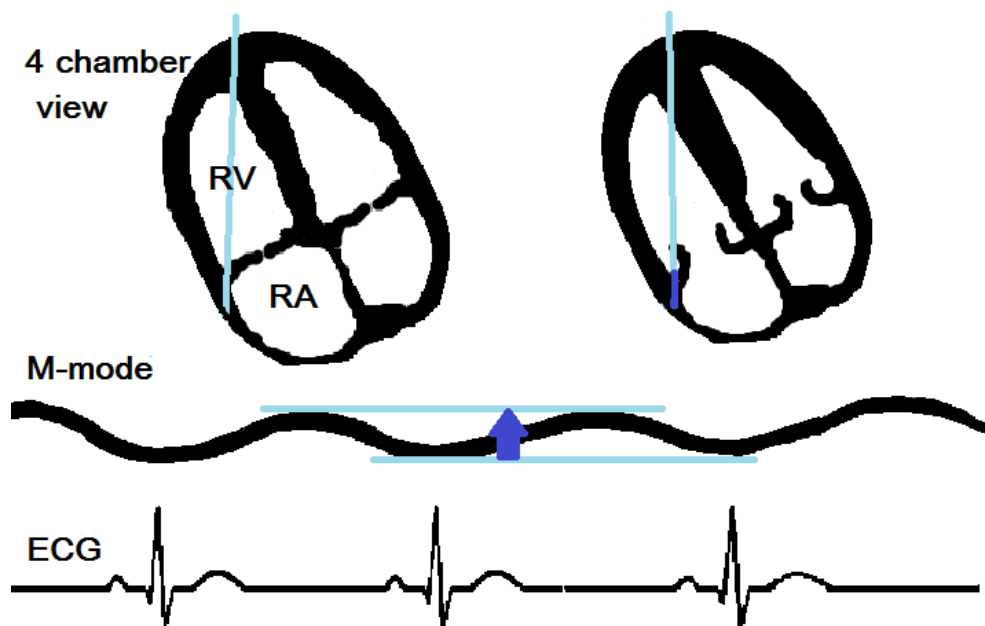


Figure 11: Tricuspid annular plane systolic excursion (TAPSE). The tricuspid valve is located between the right atrium (RA) and right ventricle (RV). Movement of the tricuspid annular plane during systole is a parameter of right heart function. TAPSE is measured in 4 chamber view. The distance between enddiastolic and endsystolic tricuspid annular plane is quantified in M-mode (blue arrow). Modified from echobasics.de¹⁰⁵.

3.2.1.4 Hemodynamic measurement and organ harvest

The measurement was performed 5 weeks after MCT injection (see Figure 6). Rats were anaesthetized with 5% isoflurane and then maintained with 2-3% isoflurane. The ventilation was sustained artificially by tracheotomy at a frequency of 60 breaths per minute. For the measurement of systemic arterial pressure, the left carotid artery was isolated and infiltrated with a catheter. Heparin was injected to avoid blood coagulation. Right ventricular systolic pressure was measured with a catheter in the jugular vein by right heart catheter. After hemodynamic assessment, lungs were perfused and cleaned with saline. Right ventricle (RV) and left ventricle plus septum (LV+S) were dissected

MATERIALS AND METHODS

and weighed. The left lung was fixed in 3,5 to 3,7% paraformaldehyde solution for histological studies. All manipulation on rats before cardiac arrest was kindly performed by Christina Vroom.

3.2.1.5 Degree of muscularization

Lung tissue was fixed in 3% paraformaldehyde solution. Double staining was performed with anti-von Willebrand-factor antibody (1:900) and anti α -SMA antibody (1:900) to detect muscularization of small peripheral pulmonary arteries of 20 to 50 μ m diameter. Vessels were categorized as fully muscularized, partially muscularized or nonmuscularized by using a computerized morphometric analysis system Leica Q Win (Leica Microsystems GmbH, Wetzlar, Germany). 80 to 100 intraacinar arteries were assessed in each rat.

3.2.1.6 Medial wall thickness

Lungs were cut in 5 μ m sections and after dehydration, subjected to Elastica van Gieson staining. The medial wall thickness was measured with light microscope Leica DM4B and the analytical software Leica Q Win (Leica Microsystems GmbH, Wetzlar, Germany). 80 to 100 intraacinar vessels of each lung tissue were analyzed. External vascular diameter ranged from 20-50 μ m. Media thickness was defined as the distance between internal elastic lamina and external elastic lamina. Measurements were performed 6 times per vessel and averaged. Parameter is expressed as percentage of external diameter.

3.2.2 Cell culture with human pulmonary arterial muscle cells

Two groups of human pulmonary arterial smooth muscle cells (hPASMC) were cultured. The first group of hPASMCs were obtained from patients with idiopathic pulmonary arterial hypertension (IPAH). The second group comprised healthy hPASMCs from donors and were purchased from PromoCell (Heidelberg, Germany). Donor as well as patients gave written informed consent. Tissue donation was performed according to the study protocol approved by the ethics committee ("Ethikkommission am Fachbereich Humanmedizin der Justus Liebig Universität Giessen") of the University Hospital Giessen (Giessen, Germany) in accordance with national law and with "Good Clinical Practice/International Conference on Harmonisation" guidelines (reference number 10/06). Both cell groups were raised on 100 mm dishes with 7 ml of smooth muscle growth medium until confluent up to passage 5-7. Proliferation was either stimulated by

MATERIALS AND METHODS

fetal calf serum (FCS) or platelet derived growth factor (PDGF).

3.2.2.1 Western Blot

3.2.2.1.1 Protein isolation

Medium was extracted from the dishes and cells were washed with Dulbecco's phosphate buffered saline (DPBS). DPBS was then withdrawn and dishes were placed on ice. Radioimmunoprecipitation assay (RIPA) buffer freshly mixed right before use served for lysis. 10 μ l of each PMSF, proteinase cocktail inhibitor and sodium orthovanadate was gently mixed with RIPA buffer. 250 μ l of prepared RIPA buffer were added to the dishes for 5 minutes. Cells were detached from the dishes with cell scratchers and transferred into cups. The mix of lysis buffer and cells was mixed on a vortex machine four times every five minutes. It was centrifuged at 4°C for 20 minutes with a velocity of 13.000 rpm. Supernatant was transferred into new cups and stored at -80°C.

3.2.2.1.2 Protein concentration

Protein concentration was measured with the DC Protein Assay on microplates. Bovine serum albumin standard ranged from 0.25 to 2 μ g/ μ l. Protein samples were adapted to the standards by solution (protein: water; 1 : 2.5). The protein concentration was double estimated by analysis software Magellan at 750nm.

3.2.2.1.3 Blotting

Five-fold sodium dodecyl sulfate (SDS) sample buffer was added to protein samples at the same concentration and denatured at 100°C for five minutes. Samples were loaded on gels (5 μ l for GAPDH (glyceraldehyde 3-phosphate dehydrogenase), 10 μ l for other proteins concentration) as well as 5 μ l of rainbow marker. The loaded gel was placed in a chamber with running buffer for 30 minutes at 100V. After samples passed the border from stacking to separating gel, voltage was augmented to 130V for another hour. After that, the gel was placed on nitrocellulose membrane and covered on both sides with blotting paper. Chambers were then filled with running buffer. Voltage was at 100V for one hour. After transfer, milk was added to the membrane for one hour. Then primary antibody was incubated overnight at 4°C. On the next day the membrane was washed with tris-buffered saline and tween (TBST) three times for six minutes followed by incubation with the secondary antibody for one hour. Membranes were washed again

MATERIALS AND METHODS

with TBST three times for six minutes and developed with Enhanced chemiluminescence (ECL) kit.

Table 3: SDS sample buffer

SDS sample buffer	Final concentration
Tris-Cl	375 mM
SDS	10% (w/v)
Glycerol	50% (w/v)
b-Mercaptoethanol	13 % (w/v)
Bromphenol blue	0,02% (w/v)

Table 4: Running buffer

Running buffer	Final concentration
Tris-HCl	25 mM
Glycin	192% (w/v)
SDS 10% (w/v)	0.1% (w/v)

Table 5: Blotting buffer

Blotting buffer	Final concentration
Tris-HCl	25 mM
Glycin	80 mM
Methanol	20% (w/v)
Aqua dest.	80% (w/v)

Table 6: Stacking gel

Stacking gel	Final concentration
Tris-Cl (0.5M)	125 mM
Acrylamide 30%	6% (w/v)
SDS 10%	0.10% (w/v)
Ammonium persulfate 10%	0.05% (w/v)
Tetramethyl ethylenediamine (TEMED)	0.10% (w/v)
H2O	

MATERIALS AND METHODS

Table 7: Separating gel

Separating gel	Final concentration
Tris-Cl (1.5M)	375 mM
Acrylamide 30%	10% (w/v)
SDS 10%	0.10% (w/v)
Ammonium persulfate 10%	0.05% (w/v)
TEMED	0.10% (w/v)
H ₂ O	

Table 8: nonfat milk

Nonfat milk	Final concentration
Milk powder	5% (w/v)
Solved in 1xTBST	

Table 9: TBST

1xTBST	Final concentration
Tris-HCl	20 mM
NaCl	137 mM
Tween	0.1% (w/v)

3.2.2.2 Proliferation assay

To measure proliferation, hPASMCs from IPAH patients and donors were seeded on 24-well plates at a concentration of 1×10^4 cells per well. The following day, cells were rendered quiescent by the addition of DMEM/F12 (0.1% FBS). After 24h, cells were forced into cell cycle reentry with 10% FBS. Different concentration of the PDE10 inhibitor were added to both IPAH and donor cells for 24 hours. 20 μ Ci [³H]-thymidine (0.02 μ Ci/ml) was given to each well for incorporation into the DNA for another 4 hours. Then cells were washed twice with 500 μ l chilled HBSS. After washing, cells were fixed by 250 μ l methanol for 15 minutes at 4°C and precipitated by 250 μ l 10% trichloroacetic acid (TCA) for 15 min at 4°C. Cells were washed with water and then lysed in 0.1 M

MATERIALS AND METHODS

NaOH. The final lysate was transferred into 4 ml scintillation solution. Assessment by scintillator gave CPM value. Proliferation assays were kindly performed by Dr. X. Tian.

3.2.3 Statistical Analysis

Prism graph pad was used for statistical analysis. Data is expressed as mean and standard error of the mean (SEM). Statistical analysis was performed with Student's t-test or one-way ANOVA for two or multiple groups, respectively. Difference between groups is regarded as significant for $P < 0.05$.

4 Results

4.1 Effect of phosphodiesterase 10 inhibition on human pulmonary arterial smooth muscle cell proliferation and signaling

4.1.1 Characterization of phosphodiesterase 10 induced proliferation in human pulmonary arterial smooth muscle cell

To characterize phosphodiesterase 10 (PDE10) induced proliferation in human pulmonary arterial SMCs we performed a proliferation assay with fetal calf serum (FCS) and platelet derived growth factor (PDGF). Both stimulators induced proliferation of human pulmonary arterial smooth muscle cells (hPASMC). PASMCs from PAH patients turned out to be more proliferative than donor arterial SMCs. By inhibition of PDE 10 with the new inhibitor PF-3188212, a dose-dependent reduction of proliferation (figure 12 and 13) was achieved. The effect began at a dose of log-10 to log-7 molar of PDE10 inhibitor and reaches the normal level at log-6 to log-5, in both FCS and PDGF stimulated cells.

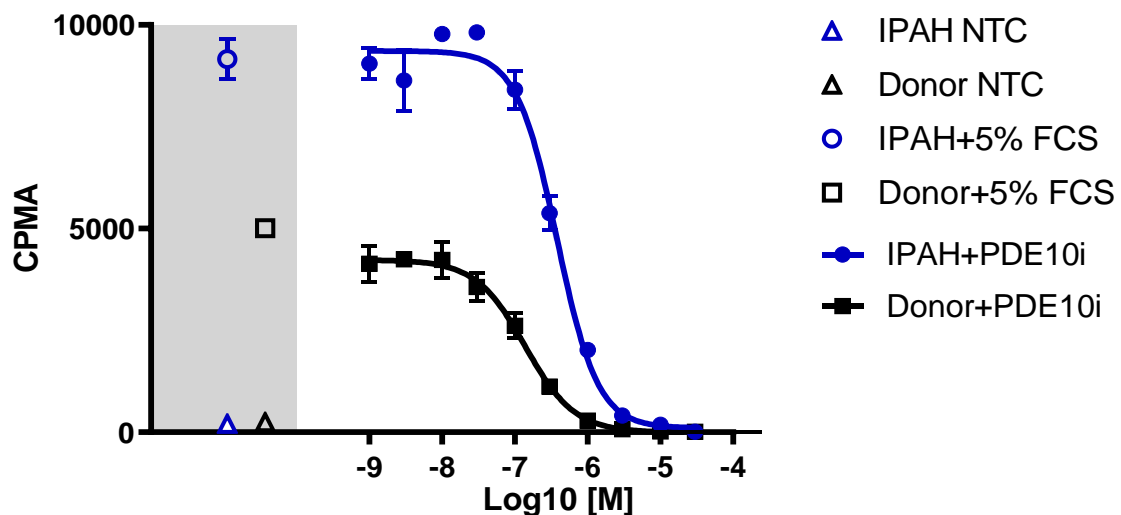


Figure 12: FCS-induced cell proliferation of hPASMC. Thymidine-uptake of hPASMC (black) and donor cells (blue) under 5%FCS stimulation for 24h hours. Inhibition of PDE10 (filled pattern) in doses from log 10 -9 to log 10 -4. [³H]-Thymidine incorporation was shown with CPMA.

RESULTS

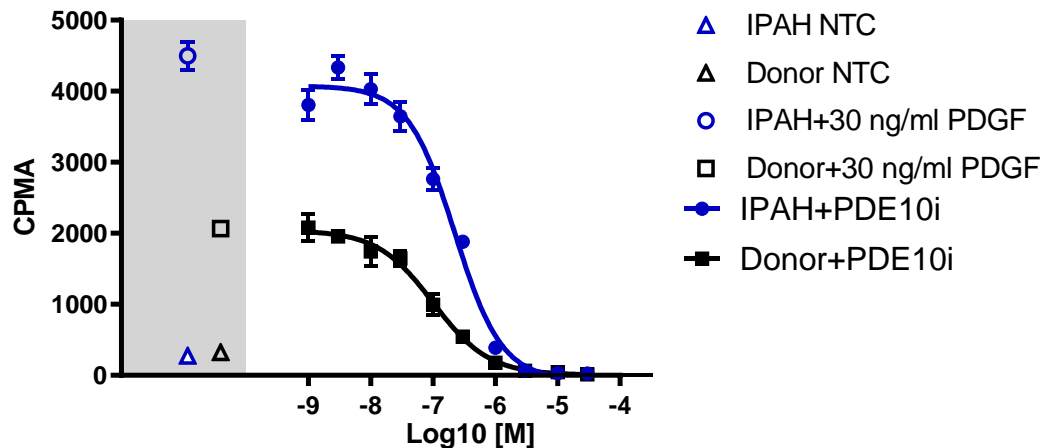


Figure 13: PDGF-induced cell proliferation of hPASMC. Thymidine-uptake of hPASMC (black) and donor cells (blue) under 30ng/ml PDGF stimulation for 24 hours. Inhibition of PDE10 (filled pattern) in doses from log 10 -9 to log 10 -4. [³H]-Thymidine incorporation was shown with CPMA.

PASMCs from PAH patients are more proliferative than donor cells. The new PDE10 inhibitor, PF-3188212, effected a dose dependent reduction of proliferation.

4.1.2 Effect of phosphodiesterase 10 inhibition on cell cycle in human pulmonary arterial smooth muscle cells

To see the molecular mechanisms that mediate PDE10 induced proliferation, western blots with cell cycle regulating proteins were performed. Of primary interest is the possible reversibility of these promoters of proliferation by inhibition of PDE10.

4.1.2.1 Influence of phosphodiesterase 10 on P27 and P21

P27 is a cyclin-dependent kinase inhibitor, and interacts with cyclin D and cyclin E. Low levels are found in cancer cells and are associated with high proliferation. For hPASMC we also can see a decreased level of p27 if stimulated with PDGF. PDE10 inhibition results in an increase to normal values.

P21, another cyclin-dependent kinase inhibitor, mediates p53-dependent cell cycle arrest. It has previously been found to be increased by PDE inhibition^{101,106}. Also, here we can see a slight increase by PDE10 inhibition with the new inhibitor. For cyclin D a

RESULTS

marked increase by stimulation with FCS is noted. PDE10 inhibition slightly reduced increase of cyclin D (Figure 14).

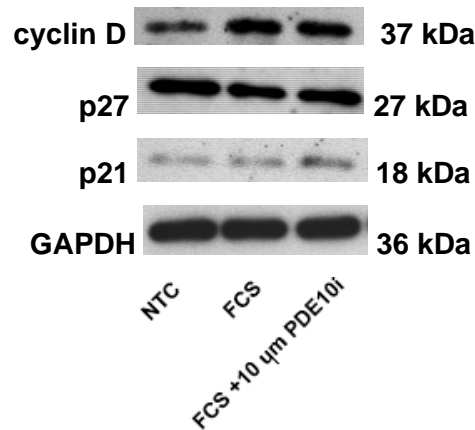


Figure 14: Influence of PDE10 on p27, p21 and cyclin D. One time immunoblot, PASM cells from IPAH patients were cultured without growth factor as non-treated cells (NTC) or stimulated with 5% FCS for 24 h (FCS). A portion of the of FCS-stimulated cells was treated with 10 μ M PDE10 inhibitor (FCS + 10 μ m PDE10i).

4.1.2.2 Cyclin D1 modulation by phosphodiesterase 10 inhibition in human pulmonary arterial smooth muscle cells

Cyclin D1 is a protein which regulates the cell cycle. It promotes progression from G1 phase to S phase and thus proliferation¹⁰⁷. PASM cells from IPAH patients were stimulated either with PDGF or with FCS. Both stimulations showed an increase in cyclin D1 concentration (shown as ratio of non-treated cells (NTC) vs PDGF group). PDE 10 inhibition reversed the significant increase of cyclin D in FCS (data not shown) and PDGF group (Figure 15).

RESULTS

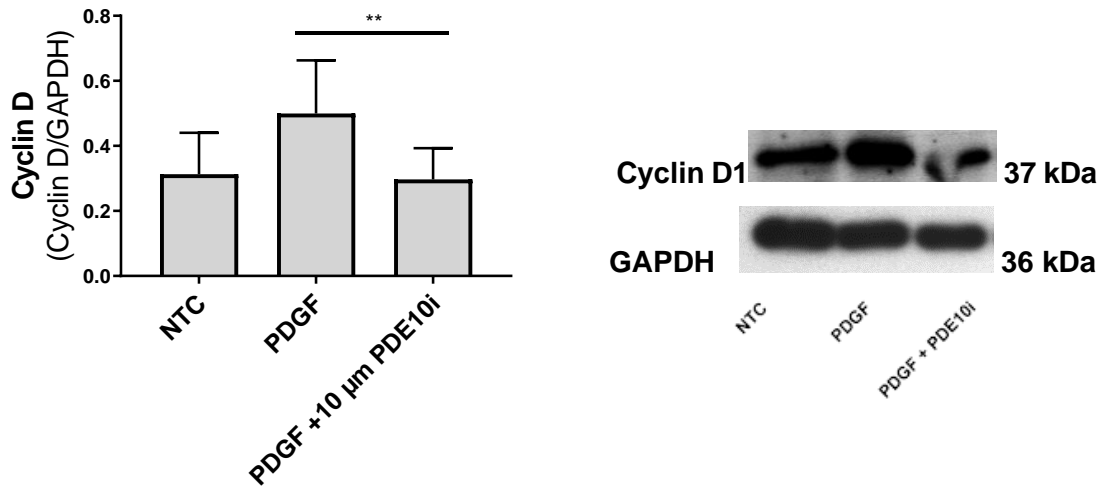


Figure 15: PDE10 inhibition reverses PDGF-induced stimulation of cyclin D in hPASMCs. PASMC of IPAH patients were cultured without growth factor (NTC) or stimulated with 30ng/ml PDGF for 2 h (PDGF). Additional inhibition with 10 μM PDE10 inhibitor was performed (PDGF+PDE10i). Representative blots are shown. GAPDH was used as loading control. Values expressed as ratio of NTC as mean ± SEM, n=2 in each group, ** p<0.01 PDGF vs PDGF+PDE10i.

4.1.3 Protein kinase A/cAMP element binding protein-axis

In many cells, cAMP levels can be increased by inhibition of PDEs. One important downstream target of cAMP is cAMP-response element-binding protein (CREB), which is activated by phosphorylation. CREB phosphorylation can be induced by the direct cAMP stimulator forskolin (data not shown). The same effect is achieved by inhibition of PDE 10 (Figure 16). PDE 10 inhibition was performed with 1 μM and 10 μM PDE inhibitor. The concentration of phosphorylated CREB showed a significant increase by inhibition with PDE 10 inhibitor at a dose of 10 μM.

CREB phosphorylation is mediated by high cAMP levels. In detail, increase of cyclic nucleotide results in activation of protein kinase A (PKA). PKA itself phosphorylates CREB. By inhibition of PDE10 with the new inhibitor PF-3188212, this axis is activated in PASMC of IPAH patients.

RESULTS

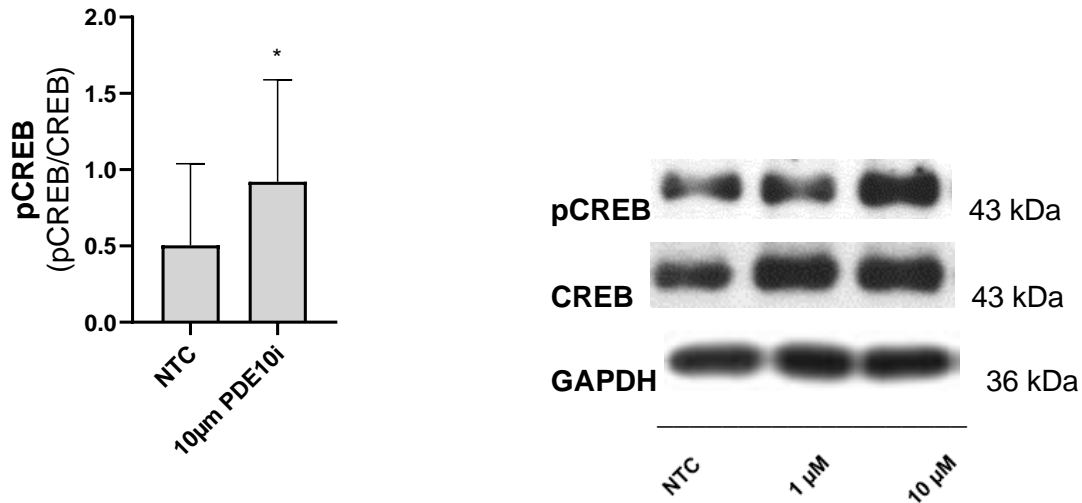


Figure 16: Increase of pCREB by PDE10 inhibition. PASMC from IPAH patients were cultured without additional growth factor. NTC = untreated hPASMCs; 1 µM = hPASMCs treated with 1 µM PDE10 inhibitor; 10 µM = hPASMCs treated with 10 µM PDE10 inhibitor; n = 3 in each group; GAPDH was used as loading control, given as ratio of pCREB vs CREB; values expressed as mean ± SEM; * p < 0.05; Representative blots are shown.

4.1.3.1 Protein kinase A and cAMP-response element binding activation via phosphodiesterase 10 inhibition in human pulmonary arterial smooth muscle cell

Via inhibition of PDE10, PKA concentration is increased significantly (Figure 17).

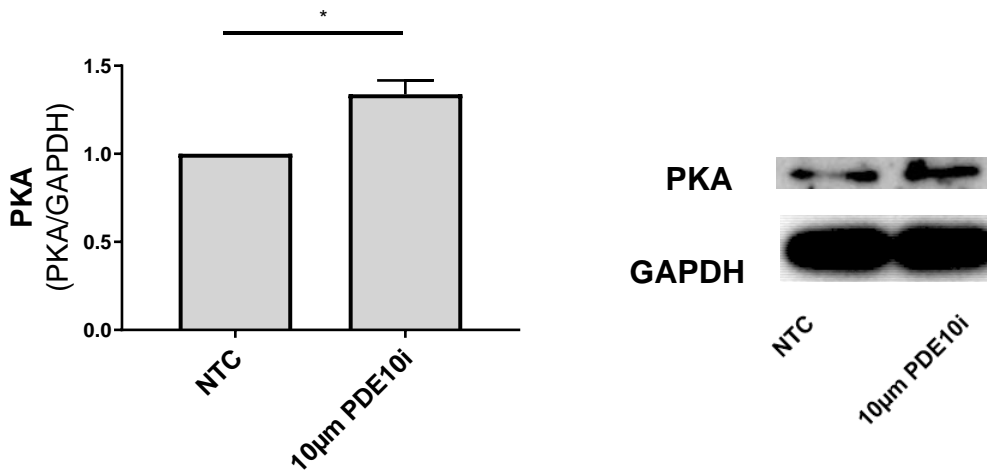


Figure 17: Increase of PKA by PDE10 inhibition. PASMC from IPAH patients were cultured without additional growth factor. NTC = untreated hPASMCs; 10 µM PDE10i = hPASMCs treated with 10 µM PDE10 inhibitor; GAPDH was used as loading control, normalized to NTC; n = 2 in each group; values are expressed as mean ± SEM; * p < 0.05.

RESULTS

4.1.3.2 Peroxisome proliferator-activated receptor γ in human pulmonary arterial smooth muscle cell

Peroxisome proliferator-activated receptors (PPAR) are nuclear proteins that function as transcription factors¹⁰⁸ and are primarily abundant in adipose tissue. Recently, PPAR γ agonism has been shown to reverse monocrotaline (MCT)-induced PAH in rats¹⁰⁹. In comparison to donor cells, PPAR γ expression is decreased in IPAH cells. By PDE10 inhibition, a non-significant increase is noted in both IPAH and donor groups.

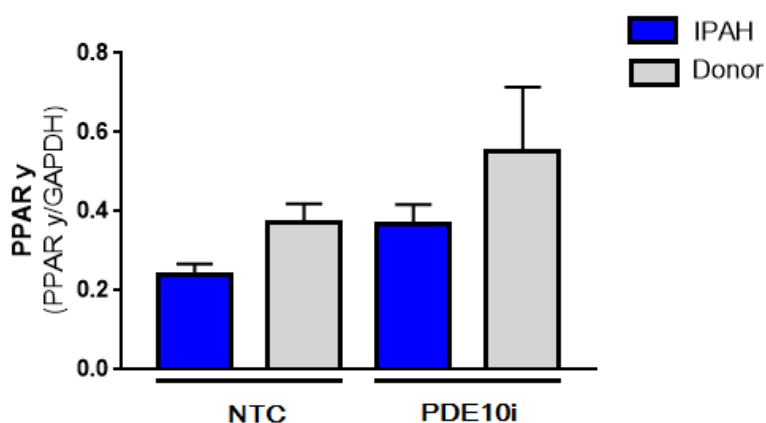


Figure 18: PPAR γ expression in hPASMC from donor and IPAH patients. Blue bars = cells from IPAH patients, grey bars = cells from donor. Inhibition of PDE 10 with 10 μ M. n=2 in each group, GAPDH was used as loading control, values expressed as mean \pm SEM, difference is not significant.

4.2 Effect of phosphodiesterase 10 inhibition in monocrotaline rat model

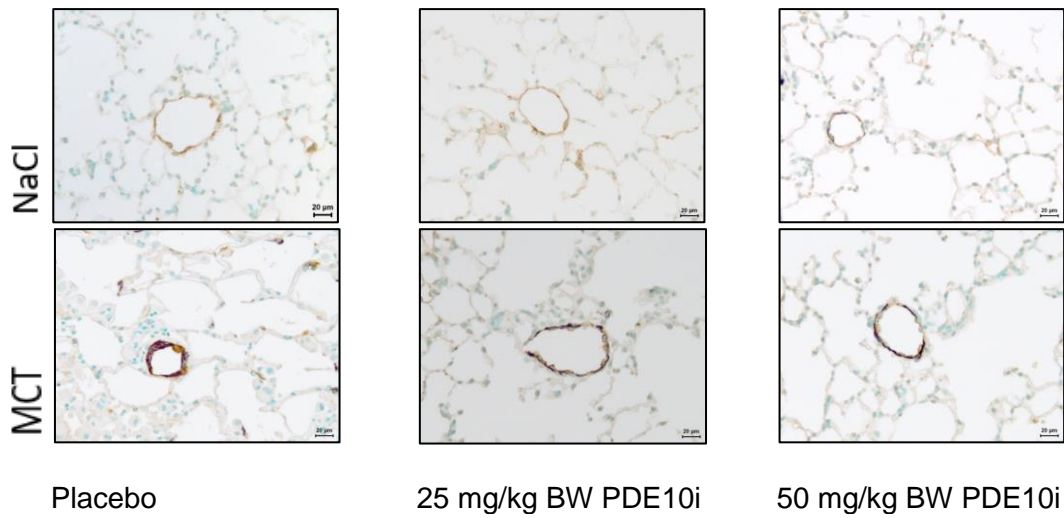
4.2.1 Histological assessment of treatment effect of phosphodiesterase 10 inhibition

4.2.1.1 Muscularization of peripheral arteries

Pulmonary hypertension results in vascular remodeling. Muscularization of peripheral arteries is one morphological pattern of PAH⁴⁹. One can divide muscularization in three different groups: nonmuscularized, partially muscularized and fully muscularized. Normal peripheral arteries are mostly nonmuscularized. In all control groups nonmuscularized arteries were over 50% (placebo: 68+11,8%, 25 mg/kg BW: 57,5+12,6%, 50 mg/kg BW: 54,8+11,8%). A smaller percentage is partially muscularized, whereas fully muscularized arteries were constantly under 5%. In MCT rats, the degree of muscularization significantly increased.

RESULTS

A)



B)

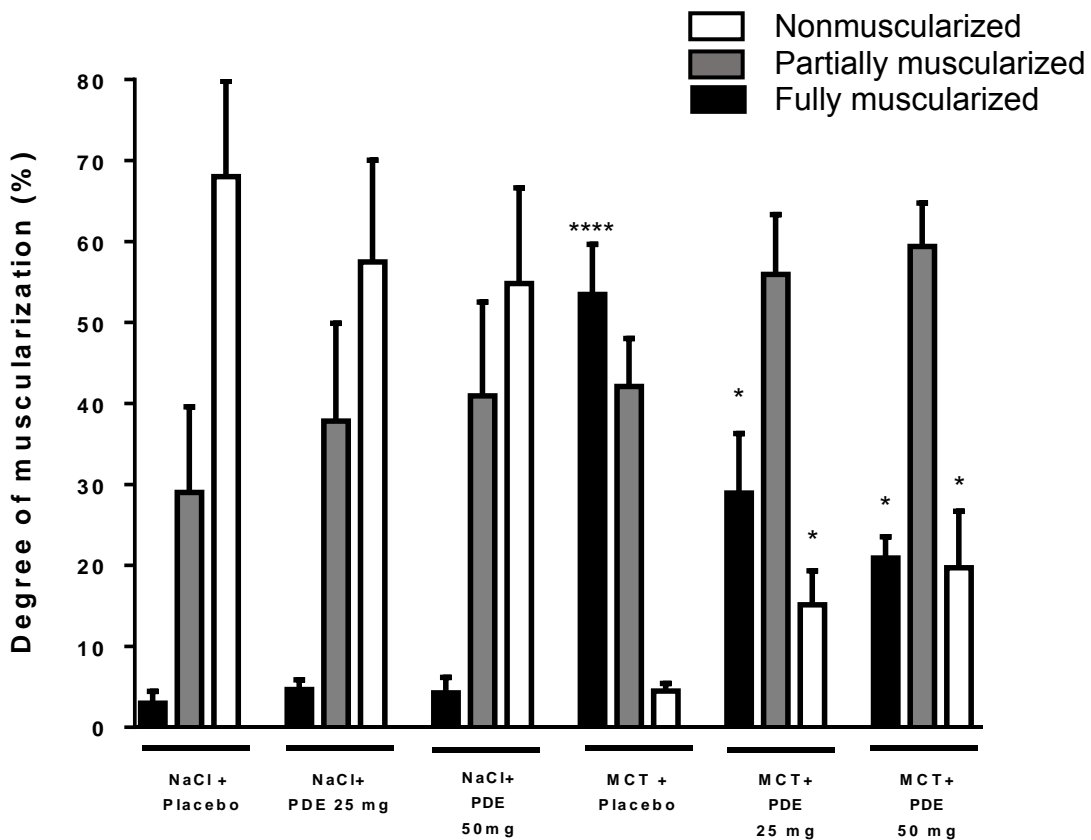


Figure 19: Effect of PDE10 inhibition on degree of muscularization. 100 intra-acinar vessels of each lung were analyzed in healthy control (NaCl) and monocrotaline (MCT) rats. PDE10 inhibitor (mg/kg BW) or placebo was applied from day 21 to day 35 orally once per day **A)** Representative pictures of lung vasculature in double immunostaining. To assess extent of muscularization SMC were indicated by α SMA (purple) and endothelial cells by von Willebrand (brown) staining. **B)** Percentage of muscularization in treatment groups. NaCl/placebo: n=5;

RESULTS

NaCl/25mg: n=5; NaCl/50mg: n=4; MCT/placebo: n=6; MCT/25mg: n=5; MCT/50mg: n=8; Black bars = fully muscularized, grey bars = partially muscularized, white bars = nonmuscularized. Values expressed as mean + SEM. Fully muscularized MCT/placebo vs NaCl/placebo **** p<0.0001, fully muscularized MCT/placebo vs MCT/25mg * p<0.05, nonmuscularized MCT/placebo vs MCT/25mg * p<0.05; fully muscularized MCT/25mg vs MCT/50mg not significant, nonmuscularized MCT/25mg vs MCT/50mg not significant.

In the MCT placebo group $53,5 \pm 6,2\%$ of arteries were fully muscularized. Also, partially muscularized arteries were slightly more frequent in MCT rats than in control groups ($42,1 \pm 5,9\%$ in MCT placebo rats vs $29,0 \pm 10,6\%$ in the NaCl placebo group). In the two groups that received the PDE10 inhibitor, the amount of partially and fully muscularized arteries was still higher than in the control group, but lower compared to the MCT placebo. Also, the majority of arteries in treated MCT groups were now partially muscularized and not fully muscularized as observed in the MCT placebo group. Nonmuscularized arteries were also significantly higher in the MCT treatment groups than in the placebo group (Figure 19).

4.2.1.2 Medial wall thickness

Besides muscularization of peripheral arteries, medial wall thickening is one type of vascular abnormalities in PAH. Measurement of medial wall thickness helps to quantify the degree of remodeling and its reversal. Vessels with a diameter from 20 to 50 μm were included. Medial wall thickness of vessels from MCT rats treated with placebo was significantly thicker than of control rats treated with placebo ($40.02 \pm 4,7 \mu\text{m}$ vs $20.40 \pm 1,6 \mu\text{m}$). In the MCT group, rats treated with 50mg/kg PDE10 inhibitor had significantly thinner medial walls in comparison to MCT placebo group. For MCT rats treated with 50 mg/kg PDE10 inhibitor, no significant reduction of medial wall thickness was shown in comparison to rats treated with 25 mg/kg PDE10 inhibitor (Figure 20).

RESULTS

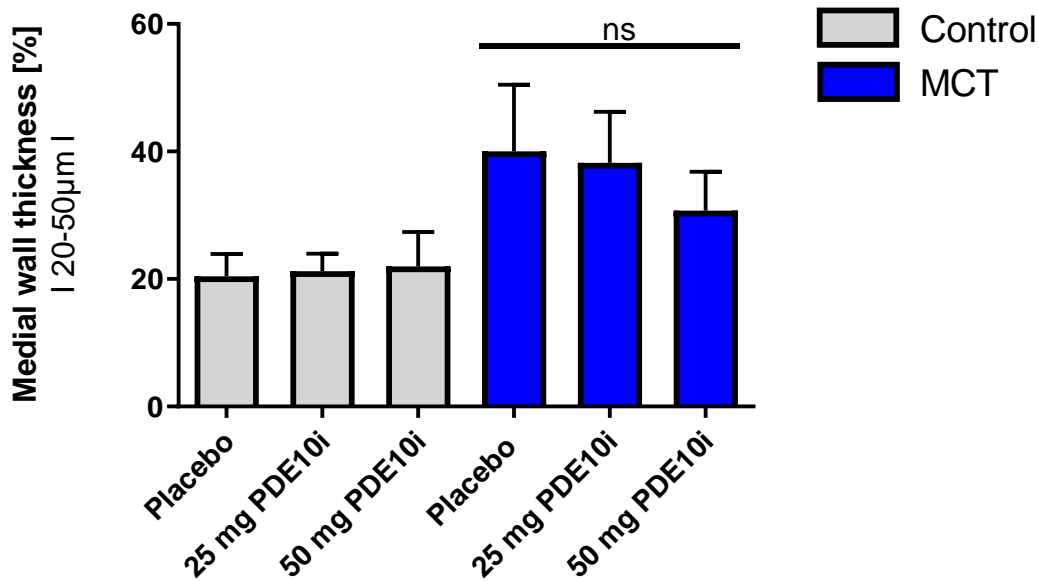


Figure 20: Medial wall thickness. Assessment of 80 to 100 intraacinar vessels with diameter from 20 – 50 μm in each lung of healthy control (grey) and MCT (blue) rats. Medial wall thickness in percentage of total diameter. PDE10 inhibitor (mg/kg BW) or placebo was applied from day 21 to day 35 orally once per day. Control/placebo: n=5; control/25mg: n=5; control/50mg: n=4; MCT/placebo: n=5; MCT/25mg: n=5; MCT/50mg: n=8; *P<0.05 MCT/placebo vs MCT/50mg.

4.2.2 Effects of phosphodiesterase 10 inhibition on hemodynamic parameters in monocrotaline rat model

An animal study was performed to assess the therapeutic effect of PDE10 inhibition. Rats were injected with MCT and control groups were injected with an equivalent volume of saline. Three weeks after MCT-injection, the pulmonary vascular system changed in ways similar to PAH. These alterations can be seen as modification in hemodynamics and even in structural changes in the right ventricle. Both parameters indicate the ongoing mechanisms in lung tissue that elevate pulmonary pressure. Indirectly, hemodynamics and right ventricle morphometry show the remodeling, vasoconstriction and thrombosis in lung vessels. Five weeks after MCT injection, hemodynamic parameters differ significantly from the control group. Right ventricular systolic pressure was markedly decreased in the MCT placebo group (Figure 21) compared with the healthy placebo group (70.1 ± 5.1 vs 32.7 ± 2.6 mmHg).

4.2.2.1 Phosphodiesterase 10 inhibition ameliorates right ventricular systolic pressure

An animal study was performed to assess the therapeutic effect of PDE10 inhibition. Five

RESULTS

weeks after MCT injection, hemodynamic parameters differ significantly relative to the control group. Right ventricular systolic pressure (RVSP) markedly increased in the MCT placebo group (Figure 21) compared with the healthy placebo group (70.1 ± 5.1 vs 32.7 ± 2.6 mmHg).

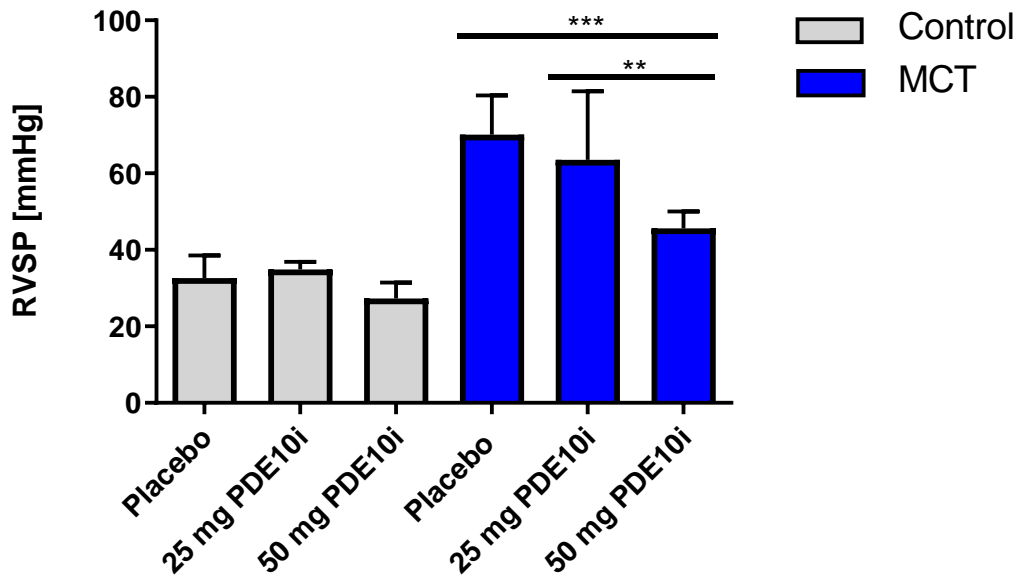


Figure 21: Effect of PDE10 inhibition on right ventricular systolic pressure on MCT-PH rats. Healthy control (grey) and MCT (blue) rats were treated with PDE10 inhibitor (in mg/kg BW) or placebo from day 21 to day 35 orally once per day. Control/placebo: n=5; control/25mg: n=5; control/50mg: n=4; MCT/placebo: n=4; MCT/25mg: n=5; MCT/50mg: n=7. Right ventricular pressure (RVSP, mmHg) is given as mean \pm SEM, **P < 0.01 MCT/25mg vs MCT/50mg, ***P < 0.001 MCT/placebo vs MCT/50mg.

Treatment with a PDE10 inhibitor for three weeks ameliorates RVSP. Whereas no significant difference in treated healthy groups is noted, RVSP is decreased by administration of PDE10i in MCT group in a dose dependent manner (70.1 ± 5.1 vs 63.6 ± 8.0 vs 45.6 ± 1.7 mmHg).

Systemic arterial pressure (SAP) was significantly lower in the MCT placebo group, while other MCT groups showed lower values without significant alteration relative to healthy groups. SAP in the MCT placebo group was significantly decreased relative to control groups and to MCT/50 mg/kg BW. MCT treated groups showed a higher SAP than MCT placebo groups, but lower SAP than all healthy groups without statistical significance (Figure 22).

RESULTS

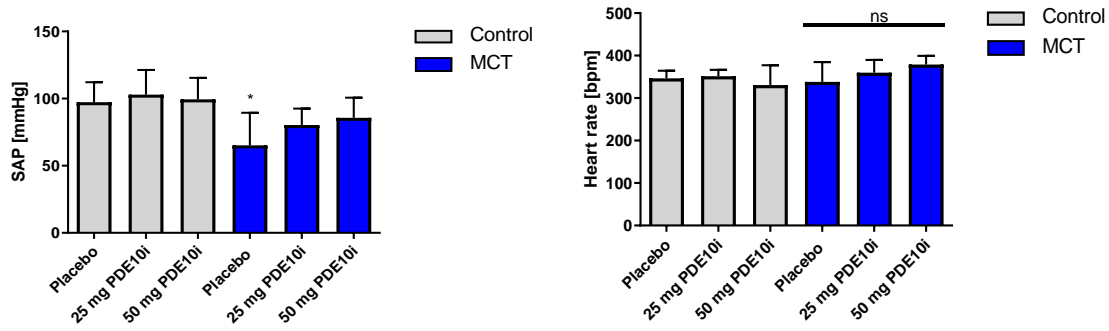


Figure 22: Systemic arterial pressure and heart rate during measurement. Healthy control (grey) and MCT (blue) rats were treated with PDE10 inhibitor (in mg/kg BW) or placebo from day 21 to day 35 orally once per day. Control/placebo: n=5; control/25mg: n=5; control/50mg: n=4; MCT/placebo: n=3 (SAP) and n=6 (heart rate); MCT/25mg: n=5; MCT/50mg: n=8. Systemic arterial pressure (SAP, mmHg), values expressed as mean + SEM, * p=0.01. Heart rate in beats per minute (bpm), ns = not significant.

4.2.3 Effect of phosphodiesterase 10 inhibition on right heart function

4.2.3.1 Tricuspid annular plane systolic excursion

The tricuspid annular plane systolic excursion (TAPSE) describes the movement of the annular plane in direction to the apex during systole. If right ventricular function is impaired, the movement is decreased. TAPSE of 20 mm in human is considered normal. Healthy control rats had a mean TAPSE of 3 mm each. For MCT rats we see a difference between treatment groups. TAPSE was generally decreased in MCT rats (Figure 23). Treatment with 25 mg/kg and 50 mg/kg PDE10 inhibitor ameliorated excursion ($2,0 \pm 0,1$ and $2,4 \pm 0,1$ mm respectively).

RESULTS

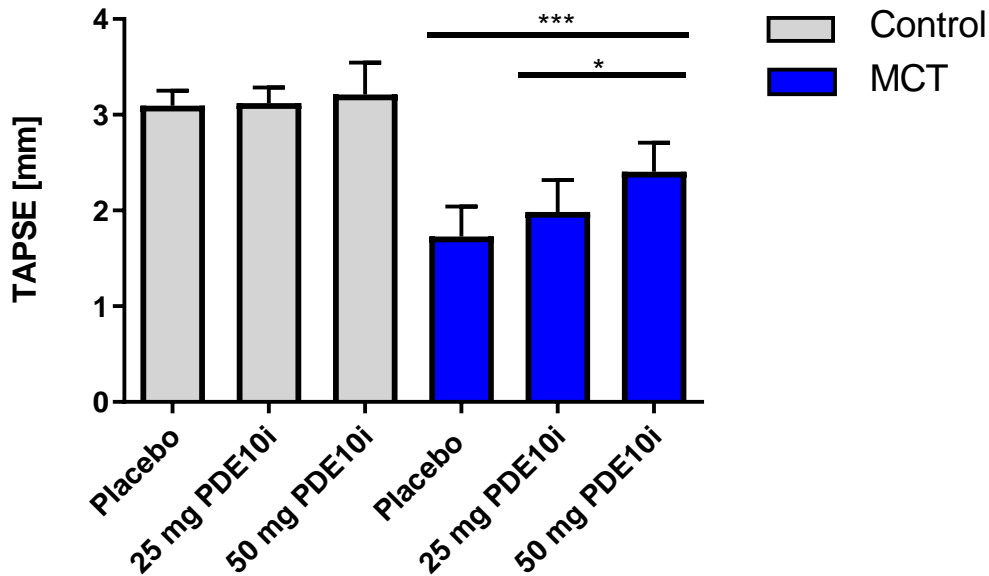


Figure 23: Tricuspid annular plane systolic excursion (TAPSE) in mm in apical 4-chamber view. Echocardiography was performed in MCT (blue) and control rats (grey) in week 5. PDE10 inhibitor (in mg/kg BW) or placebo was applied from day 21 to day 35 orally once per day. Control/placebo: n=5; control/25mg: n=5; control/50mg: n=4; MCT/placebo: n=6; MCT/25mg: n=5; MCT/50mg: n=8; *P<0.05 MCT/25mg vs MCT/50mg, *** p<0.001 MCT/placebo vs MCT/50mg.

In comparison to healthy control rats, MCT rats showed a reduced TAPSE and thus an impaired right ventricular function. PDE10 inhibition reduced impairment in a dose-dependent manner.

4.2.3.2 Phosphodiesterase 10 inhibition decreases right ventricular hypertrophy

Five weeks after MCT injection, the ratio between the mass of right ventricle (RV) and the mass of left ventricle including interventricular septum (LV+S) was calculated to assess right ventricular hypertrophy. In the MCT group, right ventricular mass was higher than in the control group. RV/LV+S ratio in the MCT placebo group was elevated in comparison to healthy placebo group. MCT administration led to right heart hypertrophy in all MCT groups (Figure 24). Right heart hypertrophy is dose dependently reduced in MCT groups treated with 25 or 50 mg/kg PDE10 inhibitor.

RESULTS

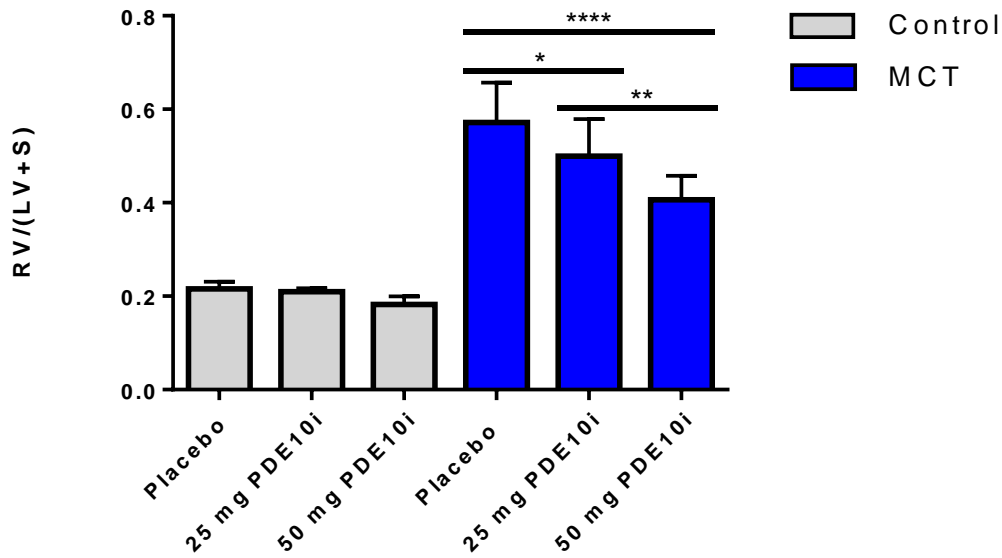


Figure 24: Effect of PDE10 inhibition on right ventricular hypertrophy on MCT-PH rats. Healthy control (grey) and MCT (blue) rats were treated with PDE10 inhibitor (in mg/kg BW) or placebo from day 21 to day 35 orally once per day. Control/placebo: n=5; control/25mg: n=5; control/50mg: n=4; MCT/placebo: n=6; MCT/25mg: n=5; MCT/50mg: n=8. RV = right ventricle, LV = left ventricle, S = septum. Ratio of RV mass divided by LV+S both in mm, expressed as mean \pm SEM, *P<0.05 MCT/placebo vs MCT/25mg, **P<0.01 MCT/25mg vs MCT/50mg, P****<0.0001 MCT/placebo vs MCT/50mg.

4.2.3.3 Cardiac index

This parameter helps to classify heart function respectively to mass. In humans, cardiac index is defined as cardiac output divided by body surface area in cm². For feasibility in rats, body weight in 100 g was used instead of body surface. Saline treated rats had a cardiac index over 20 ml/min/100g (24.9, 25.3, 24.6 ml/min per 100g BW). In the MCT placebo group, cardiac index was markedly decreased (12,5 ml/min per 100g body weight). A dose-dependent amelioration was achieved by PDE10 inhibition in MCT rats (16.5 respectively 22.0 ml/min per 100g BW).

RESULTS

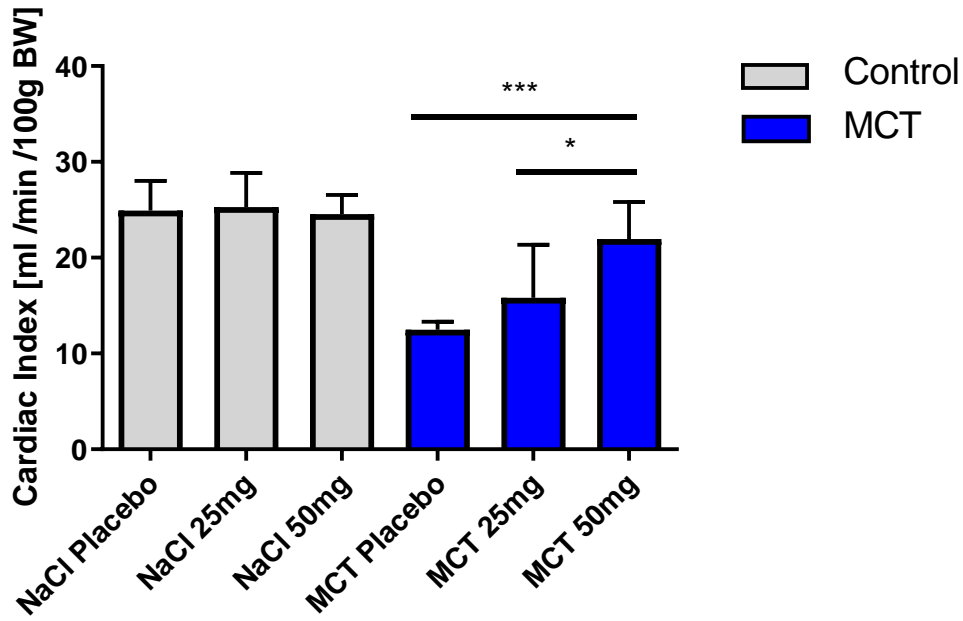


Figure 25: Cardiac Index in ml/min/100 g body weight. Healthy control (grey) and MCT (blue) rats were treated with PDE10 inhibitor (in mg/kg BW) or placebo from day 21 to day 35 orally once per day. Control/placebo: n=5; control/25mg: n=5; control/50mg: n=4; MCT/placebo: n=6; MCT/25mg: n=5; MCT/50mg: n=8. RV = right ventricle, CI= Cardiac index. Ratio expressed as mean \pm SEM, *P<0.05 MCT/25mg vs MCT/50mg, ***P<0.001 MCT/placebo vs MCT/50mg.

5 Discussion

5.1 Results

Pulmonary arterial hypertension (PAH) is a rare, but severe disease. There is still much to be learned about pathological processes contributing to PAH and of all possibilities to intervene on pathogenesis and its mediators. Phosphodiesterases (PDE), as in many other processes, play a crucial role in PAH by regulating vascular tone and even more importantly, remodeling. In addition to Endothelin-1 (ET1) antagonists and prostacyclin agonists, PDE 5 inhibitors are one of the established therapies for treatment of PAH. Other PDE isoforms like PDE1¹⁰¹, PDE2¹¹⁰, PDE3 and PDE4¹⁰⁰ show potential to ameliorate PAH in preclinical studies. The newly defined isoforms PDE7 to PDE11 are poorly investigated. Only a few studies on these new PDE members in the field of PAH exist. Interestingly, an upregulation of PDE10 in pulmonary vasculature of monocrotaline (MCT)-rats and PAH patients has been documented⁹³. PDE10 is mainly expressed in neuronal central system. Thus, it is well investigated in brain diseases as Huntington's Disease, Morbus Parkinson and Schizophrenia and shows promising effects for amelioration of these diseases in clinical studies^{96,102,103,111}. It is now time to investigate if PDE10 inhibition also has therapeutic benefits in PAH and to elucidate the mechanisms and pathways which may contribute to the role of PDE10 in PAH. For these purposes, a new, highly selective PDE 10 inhibitor (PF3188212) was used here.

5.1.1 Pulmonary arterial smooth muscle cells in patients with pulmonary arterial hypertension are hyperproliferative

Vascular remodeling is one of the pathophysiological mechanisms leading to PAH. Different cell types are involved in this process of hypertrophy and proliferation. Vascular smooth muscle cells show enormous plasticity. They can change their phenotype from a quiescent/contractile one to an active/synthetic one^{26,112}. This shift contributes to proliferation of SMC. Xia *et al.* showed, that PASMCs in the MCT rat model are more proliferative than in healthy individuals⁹³. Consistent with that finding, proliferation assays confirmed that PASMC from PAH patients are more proliferative than cells from human donors.

Smooth muscle cell proliferation leads to the common histopathological patterns medial hypertrophy and muscularization of peripheral arteries⁴⁹ and contributes to PAH. One therapeutic target to ameliorate vascular remodeling is inhibition of PDE. Cai *et al.*⁵¹

DISCUSSION

recently reported that in SMC-like cells isolated from neointima, PDE1C is significantly upregulated, and further, that inhibition of PDE1C results in reduction of proliferation by protein kinase A (PKA) mediated internalization and degradation of PDGF receptor. Stopping SMC proliferation via PDE1 and PDE 3/4 inhibition ameliorates PAH in preclinical studies^{100,101}. PDE2 inhibition was reported to show synergetic effects with PDE 5 inhibition on proliferation in PAH animals¹¹⁰.

In proliferating SMC, PDEs are known to be upregulated^{76,101}. Tian *et al.* showed an exclusive upregulation of PDE10 in PASMC of MCT rat model and reversal of SMC proliferation by PDE10 inhibition with papaverine⁹³. In this thesis PDE10 levels were investigated in human PASMC. PDE10 was upregulated in PASMC from PAH patients in comparison to healthy donors. Even though upregulation was not significant, the influence of PDE10 on PAH could be shown by inhibition with PF-3188212 that reversed PDGF-induced proliferation dose-dependently.

5.1.2 Molecular mechanisms mediating phosphodiesterase 10-induced proliferation

Hyperproliferation in human pulmonary arterial smooth muscle cells (hPASMC) is, at least by part, governed by PDE isoforms^{76,100,101}. Regulation of proliferation is mediated by cyclic nucleotides and further downstream targets. PDEs control cyclic nucleotide levels⁷⁷. PDE10 can hydrolyze both cAMP and cGMP⁹². Since PDE10 is a cAMP-inhibited cGMP hydrolyzing PDE⁹⁰, the focus of this investigation was set on the cAMP pathway, even though the influence of cGMP cannot be ruled out.

Various antiproliferative effects of cAMP in PAH are documented¹¹⁰. Activated by the growth factor PDGF, mitogen-activated protein kinase (MAPK) signaling promotes proliferation. In this case cAMP can act as a negative feedback mechanism in SMC when cyclooxygenase 2 is available^{113,114}. Further levels of cell cycle regulating proteins are increased by cAMP: P53, an anti-oncogene, and P21 stop proliferation¹¹⁵.

In addition, cell cycle protein cyclin D1 in human arterial SMC is controlled by cAMP^{106,113}. Cyclin D1 mediates progression to G1-phase and thus promotes proliferation¹⁰⁷. cAMP was found to decrease expression of cyclin D1 in rat and rabbit vascular SMC¹⁰⁶. Consistent with that, PDE10 inhibition by PF-3188212 also reduced PDGF-induced cyclin D1 increase in human PASMC.

The antiproliferative effects of PDE inhibition are further promoted by cyclic nucleotide downstream proteins¹¹⁶. The most important downstream molecules of cAMP are PKA

DISCUSSION

and EPAC (exchange protein directly activated by cAMP). This current work was focused on the PKA pathway. Inhibition of PDE10 results in increased levels of PKA in hPASMNC. PKA consists of two regulatory subunits and two catalytic subunits. The catalytic subunit is known to activate cAMP-response element-binding protein (CREB) in the nucleus via phosphorylation¹¹⁷.

Phosphorylation of CREB by PDE10 inhibition with PF-3188212 is demonstrated in this work, so inhibition of PDE10 activates cAMP/PKA/CREB pathway in hPASMNC. CREB itself is a transcription factor, promoting transcription of genes containing cAMP-response elements (CRE)¹¹⁶. For human umbilical artery smooth muscle cells and human aortic smooth muscle cells, Sun *et al.*⁵² showed that cAMP/PKA/CREB pathway induces P21 transcription. As mentioned above, P21 is an inhibitor of cell cycle progression. It inhibits cyclin dependent kinases and promotes G0/G1 cell arrest. In current investigations it was shown that PDE10 inhibition activates the cAMP/PKA/CREB pathway and further suggests that P21 transcription is enhanced.

Besides CREB, peroxisome proliferator-activated receptor (PPAR) γ , is another transcription factor implicated in pulmonary hypertension¹¹⁸. PPAR γ mainly is known as a regulator of adipose tissue and therefore is being pursued as a treatment target for diabetes¹¹⁹. Expression of ligand-activated transcription factor PPAR γ was reported to be decreased in PH in human endothelial cells¹²⁰ as well as in human PASMNC¹²¹. Reduced PPAR γ level by deletion of PPAR γ caused vascular remodeling and PAH in mice¹²¹ Further, PPAR γ prohibits vasodilator imbalance^{122,123} and inflammation¹²⁴.

Bone morphogenic protein (BMP) receptor two is mutated in approximately 75% of familial cases of PAH¹²⁵. BMPII negatively regulates cell proliferation, and dysfunction of its receptor promotes PAH. Hansmann *et al.*¹²¹ showed that the nuclear transcription factor PPAR γ is an anti-proliferative factor mediated by BMP receptor II. With its downstream target apoE, BMPII-activated PPAR γ exerts antiproliferative effects.

PPAR γ was also shown to be activated by the cGMP/PKG/PPAR γ axis in rat PASMNC¹²⁶. In western blots, the amount of PPAR γ was not significantly decreased in PASMNC of PAH patients in comparison to PASMNC of donors. By inhibition of PDE10 a non-significant increase of PPAR γ in both PAH patients and donor was noted. Since PDE10 is a cAMP hydrolyzing and cAMP-inhibited cGMP hydrolyzing PDE, the effect can be caused by the cGMP pathway. Also, CREB was previously shown to regulate PPAR γ in hepatic cells¹²⁷. Despite non-significant results in this work, PPAR γ is a promising target in PAH since animal studies exist indicating PPAR γ activation to be an effective

DISCUSSION

treatment: Behringer *et al.* showed that PPAR γ agonist Pioglitazone ameliorates PAH in MCT rat model¹⁰⁹.

5.1.3 Therapeutic effect of phosphodiesterase 10 inhibition in monocrotaline rat model

Today available drugs for treatment of PAH basically target three pathways. One of these is the augmentation of cyclic nucleotide by inhibition of PDE 5. Also, some of the other isoforms, PDE 1, 2, 3 and 4 show potential to improve PAH in animal models^{100,101,110}. PDE inhibition increases cyclic nucleotides and ameliorates PAH via vasodilation and also by anti-proliferating effects⁷¹. In contrast to other PDEs, PDE 10 is sparsely investigated in PAH. Until now, only one study on treatment effects in animal model exist⁹³. Amelioration of right ventricular systolic pressure and pulmonary vascular resistance index was shown by inhibition of PDE10 with papaverine in MCT rat model. Since selectivity of papaverine is low, in this study a new inhibitor PF-3188212 with higher selectivity was used. After 14 days, the MCT group developed PAH-typical pathologies. Treatment effects on MCT rat model was documented in different ways. Structural assessments showed significant amelioration of MCT-induced PAH. The amount of fully muscularized peripheral arteries was reduced and the amount of non-muscularized vessels increased. Medial wall thickness of peripheral arteries was enhanced as well. Given that these patterns markedly contribute to a higher vascular pressure in the lung, hemodynamic parameters were also improved by inhibition of PDE10. Right ventricular systolic pressure was significantly decreased in treatment groups and hypertrophy of the right ventricle was reduced. While these parameters were ameliorated in MCT group with treatment, heart rate and blood pressure were similar in both MCT and control groups. Inhibition by PF-3188212 showed good treatment effects and partially reversed PAH in the MCT rat model. Taken together, PDE10 might be a new treatment target in PAH.

In the last years, only few new treatment opportunities were introduced. One of them is the first oral active prostacyclin analogue Selexipag. Available since 2016¹⁹ Selexipag can be used as monotherapy or combined with PDE 5 inhibitors. In 2014 Riociguat, a soluble guanulate cyclase stimulator, was introduced⁷³. The biggest advantage of riociguat is the NO independent stimulation of guanulate cyclase. Showing good treatment effects in MCT rat model, PDE 10 should be further investigated as a promising

DISCUSSION

therapy in PAH. Since PDE10 has been investigated in neuronal diseases, there already exists a phase one study on a PDE10A inhibitor, reporting good tolerability¹¹¹.

5.2 Limitations

Animal models in PAH research serve to imitate ongoing pathogenetic processes. Rats and mice are the most used species. MCT injection, application of VEGF inhibitors, hypoxia and increased flow by pneumonectomy all can induce PAH. A combination of these pharmaceutical and physiological methods can provide a more precise picture of the disease¹²⁸. The MCT-rat model besides the hypoxia mouse model is one of the most frequently used animal models in PH. Monocrotaline is an alkaloid plant toxin, retrieved from the seams of *Crotalaria spectabilis*. After activation in the liver by oxidases to reactive alkalyzing compounds, these pyrrolic dehydro-alkaloids directly reach the lung vessels. Thus, impairment of other tissues is unlikely. The exact pathophysiological process of how MCT induces PAH-like condition is unknown. It is believed that toxic MCT initially harms endothelial cells leading to increased permeability, interstitial edema and recruitment of macrophages. This trigger might induce vascular remodeling implicating endothelial degeneration or hypertrophy, muscular hypertrophy in the medial layer and hyperplasia in adventitia. Consequently, vascular pressure is increased and right heart hypertrophy develops. These structural changes are seen two weeks after MCT-injection.

An advantage of the MCT model is the activation of toxicity in the liver and direct damage of lung vascular vessels without affecting peripheral vasculature. The highest alterations of remodeling are noted in increased media of muscularized arteries and muscularization of non-muscular arteries. So, an elevated vascular pressure is induced, analogous to naturally developed PH. Although MCT leads to pulmonary vascular remodeling, not all histological patterns are present. Plexiform lesions, the typical histological pattern in PAH, are not seen in MCT-rat model. Similar to the PAH, also in the MCT-rat model, pulmonary vascular remodeling causes increased pulmonary pressure and changes in hemodynamics. Right heart hypertrophy is the corollary of chronic increased pulmonary vascular pressure and is presented by MCT model. After passing the lung vessels, MCT reaches the heart. Up to now, there are no hints suggesting that MCT has a direct impact on myocardial muscle. But, of course, an affection of the heart by MCT cannot be fully excluded. Although the MCT-rat model provides good similarities in histology and hemodynamics, it can never fully recapitulate the human pathobiology.

5.3 Conclusion and perspectives

This study provides evidence for PDE10 as a therapeutic target in PAH. It reports a treatment effect of a new, highly specific PDE10 inhibitor, PF-3188212 in the MCT rat model. Benefit is demonstrated in structural analysis and hemodynamic parameters. Developed right ventricular hypertrophy in MCT rats was reduced by PDE10 inhibition. Since PDE10 inhibition partially reversed pulmonary remodeling and reduced right ventricular systolic pressure, myocardial benefits most likely are due to normalized pulmonary pressure. To find out if PDE10 inhibition also has direct influence on myocardial remodeling, further investigations on right heart function are needed. Pulmonary arterial banding for creation of isolated right heart insufficiency can be used to examine the isolated effects of PDE10 inhibition on right heart function. Since right heart impairment is forced by increased pulmonary pressure due to physical banding and not due to pulmonary vascular remodeling, the pharmacological effects of MCT on myocardium can be investigated in this study concept.

Given this is a preclinical study, present results only demonstrate treatment effects. Validation on safety must be performed in further studies. Being well investigated in neuronal diseases, one clinical study on PDE10 safety has been conducted, and it showed good tolerability¹¹¹.

To our knowledge, this is the first documentation of PDE10 inhibition in hPASMC. Since PDE10 is a cAMP hydrolyzing and cAMP-inhibited cGMP hydrolyzing PDE, inhibition of PDE10 increases cAMP levels and activates the cAMP/PKA/CREB pathway. The results of this study suggest that anti-proliferating effects, visible as reduced muscularization and medial thickening in lung vasculature, are at least in part mediated by cAMP and its downstream targets. PDE10 is localized near the nucleus. Its inhibition increases cAMP levels and via PKA, the amount of the transcription factor CREB. When CREB binds to CREB response element (CRE) located on DNA, transcription of genes is promoted. Interestingly, in the hippocampus the majority of transcribed genes by PPAR γ also contain CRE¹²⁹. Having the same target genes might indicate that CREB and PPAR γ act synergistically. Both the cAMP/PKA/CREB pathway^{52,106} and PPAR γ ¹³⁰ lower cyclin D1 levels, increase levels of cyclin dependent kinase inhibitor P21 and consequently stop proliferation. Interaction between PPAR γ and CREB has been reported. PPAR γ has been shown to stimulate CREB in neurons^{131,132} and vice versa, CREB negatively regulates PPAR γ in hepatocytes^{127,133}. For hPASMC the interaction of PPAR γ and CREB is not yet proven and is not demonstrated in this work, but is for sure of great interest.

DISCUSSION

Since PF-3188212 is a PDE10 specific inhibitor, additive effects by the inhibition of other PDE isoforms are unlikely. Treatment effects are attributed to cAMP increase, although cGMP might also contribute to the amelioration of disease. Influence of cGMP cannot be excluded and should be further investigated.

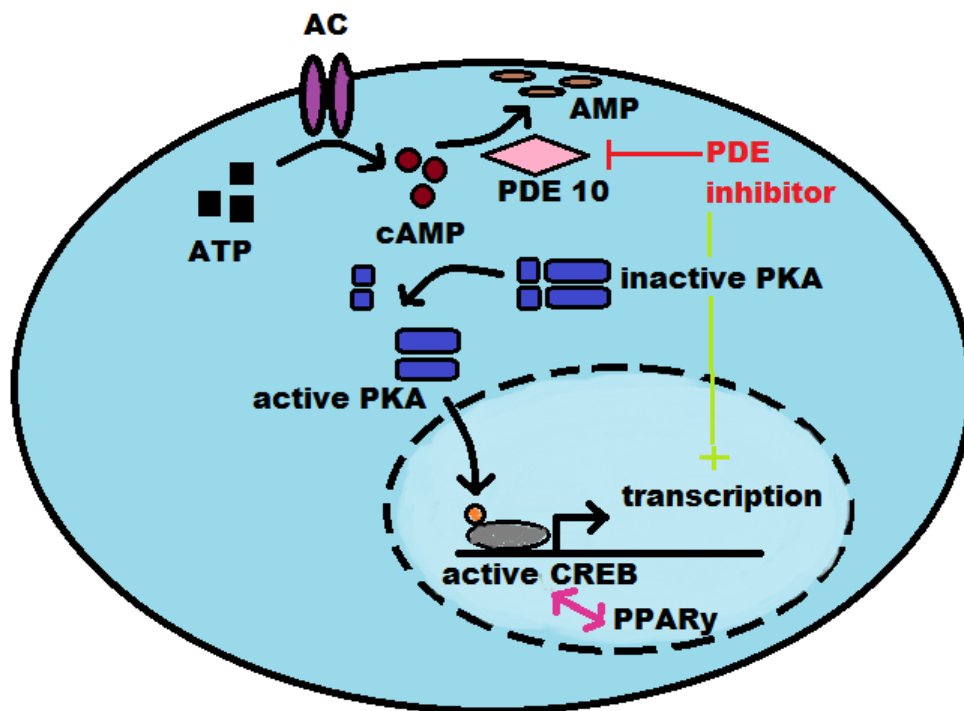


Figure 26: cAMP/PKA/CREB axis. Modified from The cAMP Pathway as Therapeutic Target in Autoimmune and Inflammatory Diseases¹³⁴. PDE 10 inhibition leads to increased level of cAMP (brown), which activates PKA (blue). Phosphorylated PKA activates CREB (orange) resulting in transcription in cell nucleus. Interaction of CREB and PPAR γ in PASMC is possible and of great interest.

Taken together, the results of this study demonstrate the potential of targeting PDE10 in PAH. To confirm these findings and enrich our knowledge concerning PDE10 and its role in PAH, more investigation on the molecular mechanisms of the cAMP pathway in PAH, the influence on the cGMP pathway and on cardiomyocytes in right heart insufficiency is needed.

6 Declaration

Erklärung zur Dissertation

„Hiermit erkläre ich, dass ich die vorliegende Arbeit selbständig und ohne unzulässige Hilfe oder Benutzung anderer als der angegebenen Hilfsmittel angefertigt habe. Alle Textstellen, die wörtlich oder sinngemäß aus veröffentlichten oder nichtveröffentlichten Schriften entnommen sind, und alle Angaben, die auf mündlichen Auskünften beruhen, sind als solche kenntlich gemacht. Bei den von mir durchgeführten und in der Dissertation erwähnten Untersuchungen habe ich die Grundsätze guter wissenschaftlicher Praxis, wie sie in der „Satzung der Justus-Liebig-Universität Gießen zur Sicherung guter wissenschaftlicher Praxis“ niedergelegt sind, eingehalten sowie ethische, datenschutzrechtliche und tierschutzrechtliche Grundsätze befolgt. Ich versichere, dass Dritte von mir weder unmittelbar noch mittelbar geldwerte Leistungen für Arbeiten erhalten haben, die im Zusammenhang mit dem Inhalt der vorgelegten Dissertation stehen, oder habe diese nachstehend spezifiziert. Die vorgelegte Arbeit wurde weder im Inland noch im Ausland in gleicher oder ähnlicher Form einer anderen Prüfungsbehörde zum Zweck einer Promotion oder eines anderen Prüfungsverfahrens vorgelegt. Alles aus anderen Quellen und von anderen Personen übernommene Material, das in der Arbeit verwendet wurde oder auf das direkt Bezug genommen wird, wurde als solches kenntlich gemacht. Insbesondere wurden alle Personen genannt, die direkt und indirekt an der Entstehung der vorliegenden Arbeit beteiligt waren. Mit der Überprüfung meiner Arbeit durch eine Plagiatserkennungssoftware bzw. ein internetbasiertes Softwareprogramm erkläre ich mich einverstanden.“

Ort, Datum

Unterschrift

7 References

1. Vonk-Noordegraaf, A., *et al.* Right heart adaptation to pulmonary arterial hypertension: physiology and pathobiology. *Journal of the American College of Cardiology* **62**, D22-33 (2013).
2. D'Alonzo, G.E., *et al.* Survival in patients with primary pulmonary hypertension. Results from a national prospective registry. *Ann Intern Med* **115**, 343-349 (1991).
3. Humbert, M., *et al.* Pulmonary arterial hypertension in France: results from a national registry. *Am J Respir Crit Care Med* **173**, 1023-1030 (2006).
4. Galie, N., *et al.* Effects of beraprost sodium, an oral prostacyclin analogue, in patients with pulmonary arterial hypertension: a randomized, double-blind, placebo-controlled trial. *Journal of the American College of Cardiology* **39**, 1496-1502 (2002).
5. Galie, N., *et al.* 2015 ESC/ERS Guidelines for the diagnosis and treatment of pulmonary hypertension: The Joint Task Force for the Diagnosis and Treatment of Pulmonary Hypertension of the European Society of Cardiology (ESC) and the European Respiratory Society (ERS): Endorsed by: Association for European Paediatric and Congenital Cardiology (AEPC), International Society for Heart and Lung Transplantation (ISHLT). *The European respiratory journal* (2015).
6. Romberg, E. *Ueber Sklerose der Lungenarterien*, (Deutsch Arch Klin Med, 1891).
7. Dresdale, D.T., Schultz, M. & Michtom, R.J. Primary pulmonary hypertension. I. Clinical and hemodynamic study. *The American journal of medicine* **11**, 686-705 (1951).
8. Simonneau, G., *et al.* Haemodynamic definitions and updated clinical classification of pulmonary hypertension. *The European respiratory journal* **53**(2019).
9. Kovacs, G., Berghold, A., Scheidl, S. & Olschewski, H. Pulmonary arterial pressure during rest and exercise in healthy subjects: a systematic review. *The European respiratory journal* **34**, 888-894 (2009).
10. Hoeper, M.M., *et al.* Definitions and diagnosis of pulmonary hypertension. *Journal of the American College of Cardiology* **62**, D42-50 (2013).
11. Gaine, S.P. & Rubin, L.J. Primary pulmonary hypertension. *Lancet* **352**, 719-725 (1998).
12. Rubin, L.J. Primary pulmonary hypertension. *N Engl J Med* **336**, 111-117 (1997).
13. Rudski, L.G., *et al.* Guidelines for the echocardiographic assessment of the right heart in adults: a report from the American Society of Echocardiography endorsed by the European Association of Echocardiography, a registered branch of the European Society of Cardiology, and the Canadian Society of Echocardiography. *J Am Soc Echocardiogr* **23**, 685-713; quiz 786-688 (2010).
14. Galie, N., *et al.* Guidelines for the diagnosis and treatment of pulmonary hypertension: the Task Force for the Diagnosis and Treatment of Pulmonary Hypertension of the European Society of Cardiology (ESC) and the European Respiratory Society (ERS), endorsed by the International Society of Heart and Lung Transplantation (ISHLT). *European heart journal* **30**, 2493-2537 (2009).
15. Luthy, E. Proceedings: The epidemic of primary pulmonary hypertension in Europe. *Pathol Microbiol (Basel)* **43**, 246-247 (1975).
16. Strange, G., *et al.* Pulmonary hypertension: prevalence and mortality in the Armadale echocardiography cohort. *Heart* **98**, 1805-1811 (2012).
17. Peacock, A.J., Murphy, N.F., McMurray, J.J., Caballero, L. & Stewart, S. An epidemiological study of pulmonary arterial hypertension. *The European respiratory journal* **30**, 104-109 (2007).

REFERENCES

18. Galie, N. & Simonneau, G. The Fifth World Symposium on Pulmonary Hypertension. *Journal of the American College of Cardiology* **62**, D1-3 (2013).
19. Sitbon, O., *et al.* Selexipag for the Treatment of Pulmonary Arterial Hypertension. *N Engl J Med* **373**, 2522-2533 (2015).
20. Pulido, T., *et al.* Macitentan and morbidity and mortality in pulmonary arterial hypertension. *N Engl J Med* **369**, 809-818 (2013).
21. Humbert, M., *et al.* Riociguat for the treatment of pulmonary arterial hypertension associated with connective tissue disease: results from PATENT-1 and PATENT-2. *Ann Rheum Dis* (2016).
22. Benza, R.L., *et al.* An evaluation of long-term survival from time of diagnosis in pulmonary arterial hypertension from the REVEAL Registry. *Chest* **142**, 448-456 (2012).
23. Galie, N., Palazzini, M. & Manes, A. Pulmonary arterial hypertension: from the kingdom of the near-dead to multiple clinical trial meta-analyses. *European heart journal* **31**, 2080-2086 (2010).
24. Hassoun, P.M., *et al.* Inflammation, growth factors, and pulmonary vascular remodeling. *Journal of the American College of Cardiology* **54**, S10-19 (2009).
25. Eddahibi, S., *et al.* Cross talk between endothelial and smooth muscle cells in pulmonary hypertension: critical role for serotonin-induced smooth muscle hyperplasia. *Circulation* **113**, 1857-1864 (2006).
26. Stenmark, K.R. & Mecham, R.P. Cellular and molecular mechanisms of pulmonary vascular remodeling. *Annu Rev Physiol* **59**, 89-144 (1997).
27. Giaid, A., *et al.* Expression of endothelin-1 in the lungs of patients with pulmonary hypertension. *N Engl J Med* **328**, 1732-1739 (1993).
28. Giaid, A. & Saleh, D. Reduced expression of endothelial nitric oxide synthase in the lungs of patients with pulmonary hypertension. *N Engl J Med* **333**, 214-221 (1995).
29. Tournier, A., *et al.* Calibrated automated thrombography demonstrates hypercoagulability in patients with idiopathic pulmonary arterial hypertension. *Thromb Res* **126**, e418-422 (2010).
30. Tudor, R.M., *et al.* Prostacyclin synthase expression is decreased in lungs from patients with severe pulmonary hypertension. *Am J Respir Crit Care Med* **159**, 1925-1932 (1999).
31. Christman, B.W., *et al.* An imbalance between the excretion of thromboxane and prostacyclin metabolites in pulmonary hypertension. *N Engl J Med* **327**, 70-75 (1992).
32. Lambers, C., *et al.* The interaction of endothelin-1 and TGF-beta1 mediates vascular cell remodeling. *PloS one* **8**, e73399 (2013).
33. Schermuly, R.T., Ghofrani, H.A., Wilkins, M.R. & Grimminger, F. Mechanisms of disease: pulmonary arterial hypertension. *Nature reviews. Cardiology* **8**, 443-455 (2011).
34. Yu, Y., *et al.* PDGF stimulates pulmonary vascular smooth muscle cell proliferation by upregulating TRPC6 expression. *Am J Physiol Cell Physiol* **284**, C316-330 (2003).
35. Hassoun, P.M. Inflammation in pulmonary arterial hypertension: is it time to quell the fire? *The European respiratory journal* **43**, 685-688 (2014).
36. Pullamsetti, S.S., *et al.* Inflammation, immunological reaction and role of infection in pulmonary hypertension. *Clin Microbiol Infect* **17**, 7-14 (2011).
37. Xu, W., *et al.* Increased arginase II and decreased NO synthesis in endothelial cells of patients with pulmonary arterial hypertension. *FASEB J* **18**, 1746-1748 (2004).
38. Herve, P., *et al.* Increased plasma serotonin in primary pulmonary hypertension. *The American journal of medicine* **99**, 249-254 (1995).

REFERENCES

39. Yuan, X.J., Wang, J., Juhaszova, M., Gaine, S.P. & Rubin, L.J. Attenuated K⁺ channel gene transcription in primary pulmonary hypertension. *Lancet* **351**, 726-727 (1998).
40. Fagan, K.A., *et al.* The pulmonary circulation of homozygous or heterozygous eNOS-null mice is hyperresponsive to mild hypoxia. *The Journal of clinical investigation* **103**, 291-299 (1999).
41. Brain, S.D., Crossman, D.C., Buckley, T.L. & Williams, T.J. Endothelin-1: demonstration of potent effects on the microcirculation of humans and other species. *J Cardiovasc Pharmacol* **13 Suppl 5**, S147-149; discussion S150 (1989).
42. Hirata, Y., *et al.* Endothelin receptor subtype B mediates synthesis of nitric oxide by cultured bovine endothelial cells. *The Journal of clinical investigation* **91**, 1367-1373 (1993).
43. Dupuis, J., Goresky, C.A. & Fournier, A. Pulmonary clearance of circulating endothelin-1 in dogs in vivo: exclusive role of ETB receptors. *J Appl Physiol* (1985) **81**, 1510-1515 (1996).
44. Rubens, C., *et al.* Big endothelin-1 and endothelin-1 plasma levels are correlated with the severity of primary pulmonary hypertension. *Chest* **120**, 1562-1569 (2001).
45. Jones, D.A., Benjamin, C.W. & Linseman, D.A. Activation of thromboxane and prostacyclin receptors elicits opposing effects on vascular smooth muscle cell growth and mitogen-activated protein kinase signaling cascades. *Mol Pharmacol* **48**, 890-896 (1995).
46. Launay, J.M., *et al.* Function of the serotonin 5-hydroxytryptamine 2B receptor in pulmonary hypertension. *Nat Med* **8**, 1129-1135 (2002).
47. Eddahibi, S., *et al.* Attenuated hypoxic pulmonary hypertension in mice lacking the 5-hydroxytryptamine transporter gene. *The Journal of clinical investigation* **105**, 1555-1562 (2000).
48. Yuan, J.X., *et al.* Dysfunctional voltage-gated K⁺ channels in pulmonary artery smooth muscle cells of patients with primary pulmonary hypertension. *Circulation* **98**, 1400-1406 (1998).
49. Rabinovitch, M. Molecular pathogenesis of pulmonary arterial hypertension. *The Journal of clinical investigation* **118**, 2372-2379 (2008).
50. Cool, C.D., *et al.* Three-dimensional reconstruction of pulmonary arteries in plexiform pulmonary hypertension using cell-specific markers. Evidence for a dynamic and heterogeneous process of pulmonary endothelial cell growth. *Am J Pathol* **155**, 411-419 (1999).
51. Cai, Y., *et al.* Role of cAMP-phosphodiesterase 1C signaling in regulating growth factor receptor stability, vascular smooth muscle cell growth, migration, and neointimal hyperplasia. *Circ Res* **116**, 1120-1132 (2015).
52. Sun, L., *et al.* Prevention of vascular smooth muscle cell proliferation and injury-induced neointimal hyperplasia by CREB-mediated p21 induction: An insight from a plant polyphenol. *Biochem Pharmacol* **103**, 40-52 (2016).
53. Rich, S., Kaufmann, E. & Levy, P.S. The effect of high doses of calcium-channel blockers on survival in primary pulmonary hypertension. *N Engl J Med* **327**, 76-81 (1992).
54. Rich, S. & Kaufmann, E. High dose titration of calcium channel blocking agents for primary pulmonary hypertension: guidelines for short-term drug testing. *Journal of the American College of Cardiology* **18**, 1323-1327 (1991).
55. Sitbon, O., *et al.* Long-term response to calcium channel blockers in idiopathic pulmonary arterial hypertension. *Circulation* **111**, 3105-3111 (2005).
56. Galie, N., *et al.* Sildenafil citrate therapy for pulmonary arterial hypertension. *N Engl J Med* **353**, 2148-2157 (2005).
57. Galie, N., *et al.* Tadalafil therapy for pulmonary arterial hypertension. *Circulation* **119**, 2894-2903 (2009).

REFERENCES

58. Jing, Z.C., *et al.* Vardenafil in pulmonary arterial hypertension: a randomized, double-blind, placebo-controlled study. *Am J Respir Crit Care Med* **183**, 1723-1729 (2011).
59. Humbert, M., *et al.* Combination of bosentan with epoprostenol in pulmonary arterial hypertension: BREATHE-2. *The European respiratory journal* **24**, 353-359 (2004).
60. Rubin, L.J., *et al.* Bosentan therapy for pulmonary arterial hypertension. *N Engl J Med* **346**, 896-903 (2002).
61. Barst, R.J., *et al.* A comparison of continuous intravenous epoprostenol (prostacyclin) with conventional therapy for primary pulmonary hypertension. *N Engl J Med* **334**, 296-301 (1996).
62. Simonneau, G., *et al.* Selexipag: an oral, selective prostacyclin receptor agonist for the treatment of pulmonary arterial hypertension. *The European respiratory journal* **40**, 874-880 (2012).
63. Montani, D., *et al.* Targeted therapies in pulmonary arterial hypertension. *Pharmacol Ther* **141**, 172-191 (2014).
64. Fan, Z., Chen, Y. & Liu, H. Calcium channel blockers for pulmonary arterial hypertension. *Cochrane Database Syst Rev*, CD010066 (2015).
65. Galie, N., *et al.* Guidelines on diagnosis and treatment of pulmonary arterial hypertension. The Task Force on Diagnosis and Treatment of Pulmonary Arterial Hypertension of the European Society of Cardiology. *European heart journal* **25**, 2243-2278 (2004).
66. Olschewski, H., *et al.* Inhaled iloprost for severe pulmonary hypertension. *N Engl J Med* **347**, 322-329 (2002).
67. Simonneau, G., *et al.* Continuous subcutaneous infusion of treprostinil, a prostacyclin analogue, in patients with pulmonary arterial hypertension: a double-blind, randomized, placebo-controlled trial. *Am J Respir Crit Care Med* **165**, 800-804 (2002).
68. Channick, R.N., *et al.* Effects of the dual endothelin-receptor antagonist bosentan in patients with pulmonary hypertension: a randomised placebo-controlled study. *Lancet* **358**, 1119-1123 (2001).
69. Galie, N., *et al.* Ambrisentan for the treatment of pulmonary arterial hypertension: results of the ambrisentan in pulmonary arterial hypertension, randomized, double-blind, placebo-controlled, multicenter, efficacy (ARIES) study 1 and 2. *Circulation* **117**, 3010-3019 (2008).
70. Keravis, T. & Lugnier, C. Cyclic nucleotide phosphodiesterase (PDE) isozymes as targets of the intracellular signalling network: benefits of PDE inhibitors in various diseases and perspectives for future therapeutic developments. *Br J Pharmacol* **165**, 1288-1305 (2012).
71. Tantini, B., *et al.* Antiproliferative effect of sildenafil on human pulmonary artery smooth muscle cells. *Basic Res Cardiol* **100**, 131-138 (2005).
72. Grimminger, F., *et al.* First acute haemodynamic study of soluble guanylate cyclase stimulator riociguat in pulmonary hypertension. *The European respiratory journal* **33**, 785-792 (2009).
73. Ghofrani, H.A., *et al.* Riociguat for the treatment of pulmonary arterial hypertension. *N Engl J Med* **369**, 330-340 (2013).
74. Galie, N., Muller, K., Scalise, A.V. & Grunig, E. PATENT PLUS: a blinded, randomised and extension study of riociguat plus sildenafil in pulmonary arterial hypertension. *The European respiratory journal* **45**, 1314-1322 (2015).
75. Conti, M. & Beavo, J. Biochemistry and physiology of cyclic nucleotide phosphodiesterases: essential components in cyclic nucleotide signaling. *Annu Rev Biochem* **76**, 481-511 (2007).
76. Wharton, J., *et al.* Antiproliferative effects of phosphodiesterase type 5 inhibition in human pulmonary artery cells. *Am J Respir Crit Care Med* **172**, 105-113 (2005).

REFERENCES

77. Beavo, J.A. Cyclic nucleotide phosphodiesterases: functional implications of multiple isoforms. *Physiol Rev* **75**, 725-748 (1995).
78. Lugnier, C. Cyclic nucleotide phosphodiesterase (PDE) superfamily: a new target for the development of specific therapeutic agents. *Pharmacol Ther* **109**, 366-398 (2006).
79. Schleicher, S., Boekhoff, I., Arriza, J., Lefkowitz, R.J. & Breer, H. A beta-adrenergic receptor kinase-like enzyme is involved in olfactory signal termination. *Proc Natl Acad Sci U S A* **90**, 1420-1424 (1993).
80. Lomas, O. & Zaccolo, M. Phosphodiesterases maintain signaling fidelity via compartmentalization of cyclic nucleotides. *Physiology (Bethesda)* **29**, 141-149 (2014).
81. Zaccolo, M., *et al.* Restricted diffusion of a freely diffusible second messenger: mechanisms underlying compartmentalized cAMP signalling. *Biochem Soc Trans* **34**, 495-497 (2006).
82. Beavo, J.A., Hardman, J.G. & Sutherland, E.W. Stimulation of adenosine 3',5'-monophosphate hydrolysis by guanosine 3',5'-monophosphate. *J Biol Chem* **246**, 3841-3846 (1971).
83. Soderling, S.H. & Beavo, J.A. Regulation of cAMP and cGMP signaling: new phosphodiesterases and new functions. *Curr Opin Cell Biol* **12**, 174-179 (2000).
84. Beavo, J.A., Conti, M. & Heaslip, R.J. Multiple cyclic nucleotide phosphodiesterases. *Mol Pharmacol* **46**, 399-405 (1994).
85. Butcher, R.W. & Sutherland, E.W. Adenosine 3',5'-phosphate in biological materials. I. Purification and properties of cyclic 3',5'-nucleotide phosphodiesterase and use of this enzyme to characterize adenosine 3',5'-phosphate in human urine. *J Biol Chem* **237**, 1244-1250 (1962).
86. Charbonneau, H., Beier, N., Walsh, K.A. & Beavo, J.A. Identification of a conserved domain among cyclic nucleotide phosphodiesterases from diverse species. *Proc Natl Acad Sci U S A* **83**, 9308-9312 (1986).
87. Charbonneau, H., *et al.* Evidence for domain organization within the 61-kDa calmodulin-dependent cyclic nucleotide phosphodiesterase from bovine brain. *Biochemistry* **30**, 7931-7940 (1991).
88. Xu, R.X., *et al.* Atomic structure of PDE4: insights into phosphodiesterase mechanism and specificity. *Science* **288**, 1822-1825 (2000).
89. Ho, Y.S., Burden, L.M. & Hurley, J.H. Structure of the GAF domain, a ubiquitous signaling motif and a new class of cyclic GMP receptor. *The EMBO journal* **19**, 5288-5299 (2000).
90. Fujishige, K., *et al.* Cloning and characterization of a novel human phosphodiesterase that hydrolyzes both cAMP and cGMP (PDE10A). *J Biol Chem* **274**, 18438-18445 (1999).
91. Loughney, K., *et al.* Isolation and characterization of PDE10A, a novel human 3', 5'-cyclic nucleotide phosphodiesterase. *Gene* **234**, 109-117 (1999).
92. Soderling, S.H., Bayuga, S.J. & Beavo, J.A. Isolation and characterization of a dual-substrate phosphodiesterase gene family: PDE10A. *Proc Natl Acad Sci U S A* **96**, 7071-7076 (1999).
93. Tian, X., *et al.* Phosphodiesterase 10A upregulation contributes to pulmonary vascular remodeling. *PLoS one* **6**, e18136 (2011).
94. Gross-Langenhoff, M., Hofbauer, K., Weber, J., Schultz, A. & Schultz, J.E. cAMP is a ligand for the tandem GAF domain of human phosphodiesterase 10 and cGMP for the tandem GAF domain of phosphodiesterase 11. *J Biol Chem* **281**, 2841-2846 (2006).
95. Siuciak, J.A., *et al.* Inhibition of the striatum-enriched phosphodiesterase PDE10A: a novel approach to the treatment of psychosis. *Neuropharmacology* **51**, 386-396 (2006).

REFERENCES

96. Schmidt, C.J., *et al.* Preclinical characterization of selective phosphodiesterase 10A inhibitors: a new therapeutic approach to the treatment of schizophrenia. *J Pharmacol Exp Ther* **325**, 681-690 (2008).
97. Bender, A.T. & Beavo, J.A. Cyclic nucleotide phosphodiesterases: molecular regulation to clinical use. *Pharmacol Rev* **58**, 488-520 (2006).
98. Murray, F., *et al.* Expression and activity of cAMP phosphodiesterase isoforms in pulmonary artery smooth muscle cells from patients with pulmonary hypertension: role for PDE1. *Am J Physiol Lung Cell Mol Physiol* **292**, L294-303 (2007).
99. Growcott, E.J., *et al.* Phosphodiesterase type 4 expression and anti-proliferative effects in human pulmonary artery smooth muscle cells. *Respir Res* **7**, 9 (2006).
100. Dony, E., *et al.* Partial reversal of experimental pulmonary hypertension by phosphodiesterase-3/4 inhibition. *The European respiratory journal* **31**, 599-610 (2008).
101. Schermuly, R.T., *et al.* Phosphodiesterase 1 upregulation in pulmonary arterial hypertension: target for reverse-remodeling therapy. *Circulation* **115**, 2331-2339 (2007).
102. Giampa, C., *et al.* Inhibition of the striatal specific phosphodiesterase PDE10A ameliorates striatal and cortical pathology in R6/2 mouse model of Huntington's disease. *PloS one* **5**, e13417 (2010).
103. Giorgi, M., *et al.* PDE10A and PDE10A-dependent cAMP catabolism are dysregulated oppositely in striatum and nucleus accumbens after lesion of midbrain dopamine neurons in rat: a key step in parkinsonism physiopathology. *Neurobiol Dis* **43**, 293-303 (2011).
104. Kojonazarov, B., *et al.* Effects of multikinase inhibitors on pressure overload-induced right ventricular remodeling. *Int J Cardiol* **167**, 2630-2637 (2013).
105. Mereles, D.
106. Vadiveloo, P.K., Filonzi, E.L., Stanton, H.R. & Hamilton, J.A. G1 phase arrest of human smooth muscle cells by heparin, IL-4 and cAMP is linked to repression of cyclin D1 and cdk2. *Atherosclerosis* **133**, 61-69 (1997).
107. Baldin, V., Lukas, J., Marcote, M.J., Pagano, M. & Draetta, G. Cyclin D1 is a nuclear protein required for cell cycle progression in G1. *Genes Dev* **7**, 812-821 (1993).
108. Ahmadian, M., *et al.* PPARgamma signaling and metabolism: the good, the bad and the future. *Nat Med* **19**, 557-566 (2013).
109. Behringer, A., *et al.* Pioglitazone alleviates cardiac and vascular remodeling and improves survival in monocrotaline induced pulmonary arterial hypertension. *Naunyn Schmiedeberg's Arch Pharmacol* **389**, 369-379 (2016).
110. Bubb, K.J., *et al.* Inhibition of phosphodiesterase 2 augments cGMP and cAMP signaling to ameliorate pulmonary hypertension. *Circulation* **130**, 496-507 (2014).
111. Tsai, M., Chrones, L., Xie, J., Gevorkyan, H. & Macek, T.A. A phase 1 study of the safety, tolerability, pharmacokinetics, and pharmacodynamics of TAK-063, a selective PDE10A inhibitor. *Psychopharmacology (Berl)* **233**, 3787-3795 (2016).
112. Owens, G.K. Regulation of differentiation of vascular smooth muscle cells. *Physiol Rev* **75**, 487-517 (1995).
113. Bornfeldt, K.E., *et al.* The mitogen-activated protein kinase pathway can mediate growth inhibition and proliferation in smooth muscle cells. Dependence on the availability of downstream targets. *The Journal of clinical investigation* **100**, 875-885 (1997).
114. Graves, L.M., *et al.* Protein kinase A antagonizes platelet-derived growth factor-induced signaling by mitogen-activated protein kinase in human arterial smooth muscle cells. *Proc Natl Acad Sci U S A* **90**, 10300-10304 (1993).
115. Hayashi, S., *et al.* Cyclic AMP inhibited proliferation of human aortic vascular smooth muscle cells, accompanied by induction of p53 and p21. *Hypertension* **35**, 237-243 (2000).

REFERENCES

116. Klemm, D.J., *et al.* cAMP response element-binding protein content is a molecular determinant of smooth muscle cell proliferation and migration. *J Biol Chem* **276**, 46132-46141 (2001).
117. Johannessen, M., Delghandi, M.P. & Moens, U. What turns CREB on? *Cell Signal* **16**, 1211-1227 (2004).
118. Pullamsetti, S.S., Perros, F., Chelladurai, P., Yuan, J. & Stenmark, K. Transcription factors, transcriptional coregulators, and epigenetic modulation in the control of pulmonary vascular cell phenotype: therapeutic implications for pulmonary hypertension (2015 Grover Conference series). *Pulm Circ* **6**, 448-464 (2016).
119. Yki-Jarvinen, H. Thiazolidinediones. *N Engl J Med* **351**, 1106-1118 (2004).
120. Ameshima, S., *et al.* Peroxisome proliferator-activated receptor gamma (PPARgamma) expression is decreased in pulmonary hypertension and affects endothelial cell growth. *Circ Res* **92**, 1162-1169 (2003).
121. Hansmann, G., *et al.* An antiproliferative BMP-2/PPARgamma/apoE axis in human and murine SMCs and its role in pulmonary hypertension. *The Journal of clinical investigation* **118**, 1846-1857 (2008).
122. Martin-Nizard, F., *et al.* Peroxisome proliferator-activated receptor activators inhibit oxidized low-density lipoprotein-induced endothelin-1 secretion in endothelial cells. *J Cardiovasc Pharmacol* **40**, 822-831 (2002).
123. Calnek, D.S., Mazzella, L., Roser, S., Roman, J. & Hart, C.M. Peroxisome proliferator-activated receptor gamma ligands increase release of nitric oxide from endothelial cells. *Arterioscler Thromb Vasc Biol* **23**, 52-57 (2003).
124. Szanto, A. & Nagy, L. The many faces of PPARgamma: anti-inflammatory by any means? *Immunobiology* **213**, 789-803 (2008).
125. Soubrier, F., *et al.* Genetics and genomics of pulmonary arterial hypertension. *Journal of the American College of Cardiology* **62**, D13-21 (2013).
126. Wang, J., *et al.* Sildenafil inhibits hypoxia-induced transient receptor potential canonical protein expression in pulmonary arterial smooth muscle via cGMP-PKG-PPARgamma axis. *Am J Respir Cell Mol Biol* **49**, 231-240 (2013).
127. Herzig, S., *et al.* CREB controls hepatic lipid metabolism through nuclear hormone receptor PPAR-gamma. *Nature* **426**, 190-193 (2003).
128. Morimatsu, Y., *et al.* Development and characterization of an animal model of severe pulmonary arterial hypertension. *J Vasc Res* **49**, 33-42 (2012).
129. Denner, L.A., *et al.* Cognitive enhancement with rosiglitazone links the hippocampal PPARgamma and ERK MAPK signaling pathways. *J Neurosci* **32**, 16725-16735a (2012).
130. Wakino, S., *et al.* Peroxisome proliferator-activated receptor gamma ligands inhibit retinoblastoma phosphorylation and G1--> S transition in vascular smooth muscle cells. *J Biol Chem* **275**, 22435-22441 (2000).
131. Makela, J., *et al.* Peroxisome proliferator-activated receptor-gamma (PPARgamma) agonist is neuroprotective and stimulates PGC-1alpha expression and CREB phosphorylation in human dopaminergic neurons. *Neuropharmacology* **102**, 266-275 (2016).
132. Liu, J., *et al.* Roscovitine, a CDK5 Inhibitor, Alleviates Sevoflurane-Induced Cognitive Dysfunction via Regulation Tau/GSK3beta and ERK/PPARgamma/CREB Signaling. *Cell Physiol Biochem* **44**, 423-435 (2017).
133. Liu, Y., *et al.* PEGylated Curcumin Derivative Attenuates Hepatic Steatosis via CREB/PPAR-gamma/CD36 Pathway. *Biomed Res Int* **2017**, 8234507 (2017).
134. Raker, V.K., Becker, C. & Steinbrink, K. The cAMP Pathway as Therapeutic Target in Autoimmune and Inflammatory Diseases. *Front Immunol* **7**, 123 (2016).

REFERENCES

*McLaughlin VV, Archer SL, Badescj DB, et al. ACCF/AHA 2009 expert consensus document on pulmonary hypertension: a report of the American College of Cardiology Foundation Task Force on Expert Consensus Documents and the American Heart Association: developed in collaboration with the American College of Chest Physicians, American Thoracic Society, Inc., and the Pulmonary Hypertension Association. *Circulation* 2009;119:2250-94.